**DOI: https://doi.org/10.24297/jap.v22i.9596**

# Design study of a disruptive self-powered power plant prototype

Ramon Ferreiro García (independent author)

Ex-Prof. Emeritus at University of A Coruna, Spain

https://www.udc.es, ,ramon.ferreiro@udc.es

**Abstract**

This research work discusses a preliminary disruptive prototype design of a self-powered thermal power plant doing work by strictly isothermal closed processes using forced convection heat transfer both for adding and extracting heat. It includes useful work by expansion and vacuum-based contraction due to adding heat to and extracting heat from a working fluid. A cycle analysis considering useful work due to vacuum-based contraction is the core of the problem-solving methodology. The findings will be applied to the prototyping implementation task, which includes the cascade and series of cascade coupling of several regenerative power units. The empirical results of the case studies provide the data needed to carry out a prototyping task considering the results of real cases subjected to realistic irreversibilities and heat recovery factors that make the self-feeding power plant an interesting design option. This extraordinary result confirms the technical viability of real machines that exhibit the ability to provide more energy than they use, that is, second-class perpetual motion machines

**Keywords**: contraction work, cooling-based work, self-powered engine, self-feeding engine, vacuum-based work.

| **Nomenclature** | |
|---|---|
| **Acronyms** | **description** |
| HTF | Heating transfer fluid |
| CTF | Cooling transfer fluids |
| TWF | Thermal working fluid |
| HRS | Heat recovery system |
| LF | Losses factor (irreversibilities): 1, no losses; 0, 100% losses |
| RF | Heat recovery factor: 1, 100% recovering effectiveness |
| HREx | Heat recovery exchanger |
| SFI | Self-feeding index |
| RIT | Ration of isothermal temperatures in cycle VTVT: $T_1/T_2$ |
| PU | Power unit |
| SPS | Self-Powered System |
| PP | Power Plant (composed by several PUs) |
| RDAC | Reciprocating double-acting cylinder |
| VTVT | Cycle composed by isochoric-isothermal-isochoric-isothermal processes |
| $VTVT_{\_reg}$ | Regenerative VTVT cycle |
| FCF | Forced convection fan |
| HS, PS | Heat source, power source, power supply |
| | |
| **Symbols/units** | **description** |
| $p$[bar] | Absolute pressure |
| $q_i$[kJ.kg$^{-1}$] | specific heat in |
| $q_o$[kJ.kg$^{-1}$] | specific heat out |
| $s$[kJ.kg$^{-1}$.K] | specific entropy |
| $T$[K] | temperature |

| | |
|---|---|
| $T_H$[K] | top temperature |
| $T_L$[K] | bottoming temperature |
| $u$[kJ.kg$^{-1}$] | specific internal energy |
| $v$[kJ.kg$^{-1}$] | specific volume |
| $V$[m$^3$] | volume |
| $w$[kJ.kg$^{-1}$] | specific work |
| $w_i$[kJ.kg$^{-1}$] | specific work in |
| $w_o$[kJ.kg$^{-1}$] | specific work out |
| $q_{i12}$ [kJ.kg$^{-1}$] | Input heat to cycle process 1-2 |
| $q_{i23}$ [kJ.kg$^{-1}$] | Input heat to cycle process 2-3 |
| $q_{i12+23}$ [kJ.kg$^{-1}$] | Input heat to cycles processes 1-2 and 2-3 |
| $q_{iext} = q_i - q_{reg34}$[kJ.kg$^{-1}$] | External heat added to the cycle |
| $q_{o34}$ [kJ.kg$^{-1}$] | Output heat to cycle process 3-4 |
| $q_{o41}$ [kJ.kg$^{-1}$] | Output heat to cycles process 4-1 |
| $q_{o34+41}$ [kJ/kg] | Output heat to cycles processes 3-4 and 4-1 |
| $q_{reg34}$ [kJ.kg$^{-1}$] | Regenerated heat extracted from cycle process 3-4 |
| $w_{oexp} = w_{o\_23}$ [kJ.kg$^{-1}$] | Output expansion work $w_{o23}$ due to added heat |
| $w_{ocont} = w_{o\_41}$ [kJ.kg$^{-1}$] | Output contraction work $w_{o41}$ due to extracted heat |
| $w_n$ [kJ.kg$^{-1}$] | Net useful work ($w_{oexp} + w_{ocont}$) = ( $w_{o23} + w_{o41}$) |
| *RF* [%] | Cycle heat recovery factor = $q_{reg34}/q_{o34}$; RF = 1, 100% recovering effectiveness; RF = 0, 0% recovering effectiveness |
| *LF* [%] | Losses factor (thermal and mechanical irreversibilities); LF=1, no losses; LF=0, 100% losses |
| *RIT* = $T_1/T_2$ | ratio of isothermal temperatures for a VTVT cycle |
| *SFI* [%] | Self-feeding index = $\eta_{th\_reg} - 100$ |
| $\eta_{th}$ [%] | Cycle thermal efficiency |
| $\eta_{th\_reg}$ [%] | Regenerative cycle thermal efficiency |
| $\eta_{th\_exp}$ [%] | Thermal efficiency of expansion process |
| $\eta_{th\_cont}$ [%] | Thermal efficiency of contraction process |
| Min_pres [bar] | Minimum cycle pressure |
| Ref_pres = $p_{ref}$ (bar) | Reference cycle pressure (initial cycle pressure) |
| Max_pres [bar] | Maximum cycle pressure |

**1 Introduction**

This paper proposes the combination of a set of already known technical contributions, which are conveniently associated and give rise to a thermal machine capable of self-generating energy without violating any conventional established thermodynamic principle. Such technical contributions mainly concern the development of design strategies necessary to avoid as much as possible some thermal and mechanical losses associated with conventional power plants operating with open processes, which entail at least the following losses due to:

1 the flow work losses inherent to the enthalpy of the thermal working fluid (TWF)

2 isentropic losses inherent to open processes

3 the heat of vaporization associated with state changes

4 state changes due to the working fluid condensation, which undergoes heat degradation so that the released heat cannot be effectively recovered

5 feed pumps working among the most common losses

Notwithstanding the foregoing, the achievement of part of the main objectives aimed at prototyping the proposed energy converter requires overcoming the above-enumerated drawbacks responsible for the main energy losses and implementing some other disruptive techniques that concern the following tentative improvements:

1. avoiding heat transfer losses by circulating the heat transfer fluid under countercurrent forced convection in closed circuit recirculation
2. systematically using of vacuum to perform useful mechanical work accomplished by cooling with heat removal at zero cost
3. using strictly isothermal closed processes, which convert 100% of the isothermal added heat into useful mechanical work
4. implementing combined strategies that give rise to an absolutely disruptive heat recovery technique whose description is developed throughout the article

The advances on which the proposed contributions are based start with the techniques of conversion of heat to work through a vacuum in open processes. Therefore, for instance, some vacuum systems change their state via the condensation of the TWF (from steam to liquid water). This can be carried out in both open and closed processes, whereby open processes correspond to Thomas Savery (1650–1715) [1], Thomas Newcomen (1664–1729) [2], and James Watt (1736–1819) [3]. J.G. van der Kooij (2015) [4] made a valuable contribution to the diffusion of steam engines based on vacuums. This contribution highlights Newcomen's atmospheric steam engine types, in which useful mechanical work is performed under vacuums by condensing the expanded steam exhausted from a cylinder. Later, Watt improved the concept of the atmospheric pressure steam engine designed by Newcomen by implementing prototypes equipped with a steam condenser located independently of the actuator cylinder.

Moreover, Alessandro Nuvolari (2004) [5] reviewed steam power technology involving water vapor by considering steam engines that were initially operated at atmospheric pressure through the thermal contraction of steam (vacuum) when it condensed through cooling by heat extraction. Later, Gerald Müller (2013) [6] presented an innovative concept concerning low-temperature-based atmospheric steam engines. The author extended the theory of the atmospheric steam engine operating under a vacuum achieved by heat extraction. In doing so, he showed that operation is possible at temperatures between 60 °C and 100 °C, although efficiency is further reduced as the temperature increases.

Similarly, Gerald Müller and George Parker (2015) [7] conducted a series of experiments to assess this theory by including a forced expansion stroke. Recently, the atmospheric steam engine (which implies that useful work is due to the presence of a vacuum) was re-evaluated. According to the authors, the theoretical efficiency of the ideal engine can be increased from 6.5% to 20%.

Three disruptive technological challenges must be overcome to implement power units (PUs) capable of being operated by thermal contraction based on a vacuum under strictly isothermal closed processes:

1. The proposed thermal machine must be able to operate with the aforementioned thermal cycle (i.e., it must be capable of operating through thermal contraction, including vacuum-based contraction).
2. The thermal cycles chosen for the proposed thermal machine must be able to operate with strictly isothermal processes of both thermal expansion and thermal contraction, which includes closed processes-based vacuum.
3. The thermal machine must be equipped with highly effective forced thermal convection heat transfer media at the transfer rate required by the nominal power of each PU. Furthermore, every PU must be composed of a pair of reciprocating double-acting cylinders (RDACs) equipped with associated heat transfer equipment. Furthermore, forced convection heat transfer is essential for achieving cooling-based contraction work through the highest possible vacuum. Consequently, a high vacuum is essential.

During the last three decades, some attempts to advance isothermal processes have been made [8–15]. Recently, Vítor Augusto Andreghetto Bortolin et al. (2021) [8] proposed a complete thermodynamic model for the adiabatic and isothermal atmospheric steam cycle that uses real gas data. The model was constructed to accommodate the forced expansion of low-pressure steam. The results show that the adiabatic cycle is more efficient than the isothermal cycle and that the amount of heat needed to keep the expanding steam at a constant temperature prohibits practical applications. In other work, Knowlen C. et al. (1997) [9] developed an automotive propulsion concept of an open Rankine cycle that utilizes liquid nitrogen as the working fluid and discussed several means of achieving quasi-isothermal expansion. The authors claim that if sufficient heat input during the expansion process can be realized, then this cryogenic propulsive system will provide greater automotive ranges and lower operating costs than those of electric vehicles currently being considered for mass production.

Meanwhile, Cicconardi S. et al. (1999) [10] studied a steam cycle and the effect of flow variation on cycle performance. The authors claim that isothermal expansion with increasing flow decreases cycle efficiency because condenser losses are increased and the full recovery of the available heat at the end of the expansion is impossible at high superheated temperatures. In other research, Cicconardi S. et al. (2001) [11] showed that isothermal expansion can achieve high efficiency (up to 70% of HHV) when the waste heat at the turbine outlet is recovered for pre-heating water, hydrogen, and oxygen.

Park J.K. et al. (2012) [12] analyzed the application of a quasi-isothermal thermal cycle in an underwater energy storage system. The analysis of the heat transfer cycle confirmed the validity of the quasi-isothermal nature of the design based on water pistons. Kim Y.M. et al. (2013) [13] reviewed current thermo-electric energy storage (TEES) systems and proposed a novel isothermal TEES system with transcritical $CO_2$ cycles. For the given efficiencies of the compressor and expander, the maximum round-trip efficiency decreased rapidly when the back work ratio was increased. The authors showed that the round-trip efficiency of the isothermal TEES system can be increased because it has a lower back work ratio than in the isentropic case.

Meanwhile, Opubo N. et al. (2013) [14] proposed a variant of a thermal engine that uses isothermal expansion to achieve a theoretical efficiency close to the Carnot limit and in which steam generated inside a power cylinder eliminates the need for an external boiler. The device is suitable for slow-moving applications, and preliminary experiments have shown a cycle efficiency of 16% and a high work ratio of 0.997. Later, Opubo N. et al. (2014) [15] reviewed various low-temperature vapor power cycle heat engines with quasi-isothermal expansion using methods to realize the heat transfer. In this experiment, the heat engines took the form of either a Rankine cycle with continuous heat addition during the expansion process or a Stirling cycle with a condensable vapor as the working fluid.

R. Ferreiro et al. [16–19] presented state-of-the-art technologies for thermal cycles that allow operation with strictly isothermal closed processes of both thermal expansion and contraction. Meanwhile, other research indicates some advances in the ability to achieve highly effective forced thermal convection heat transfer media at the required transfer rate [20–21].

During the last three decades, a great effort has been made to implement highly effective heat recovery units. For this reason, there are many studies on advanced design techniques. Of particular interest is the work of Meeta Sharma and Onkar Singh (2013) [20]. They considered the physical parameters of a heat recovery steam generator (HRSG) and studied the implications of HRSG design by comparing an existing plant design with an optimized plant design. Another relevant work is that by Meeta Sharma and Onkar Singh (2014) [21], who presented an exergy analysis of an HRSG for calculating exergy losses, heat transfer, and pressure losses for different physical components. They found that various HRSG sub-sections have different physical parameters, such as fin density, fin thickness, fin height, tube diameter, and fin spacing, and that they noticeably affect exergy loss minimization. Such information aids in designing new HRSG technologies and reducing thermal losses in existing HRSGs. Furthermore, such design strategies and advanced methodologies could be applied to design HREs to achieve prototypes with greater heat transfer effectiveness.

In Newcomen and James Watt steam engines [2-3] that operate at atmospheric pressure in the high-pressure zone and with a vacuum in the low-pressure zone, the volumetric zone of the cylinder in contact with the condenser was subjected to a pressure lower than the atmospheric pressure known as a vacuum. The work obtained by these engines was due to the generation of a vacuum by cooling via heat extraction from the condenser in an open process. The open process of cooling carried out by heat extraction responsible for this vacuum decreases entropy while providing useful mechanical work. This common phenomenon occurs in reciprocating steam engines at constant pressure, constant temperature, and change of state in open process-based transformations.

**2 Disruptive self-powered regenerative PU operating with a VTVT thermal cycle**

In all heat convertors characterized by useful mechanical work done by contraction-based compression under closed processes without state changes, the conversion of heat to useful work is carried out simultaneously by three additive techniques:

1. conversion by expansion of the TWF characterized by converting a fraction of the added heat to useful mechanical work, which absorbs heat
2. conversion by the thermal contraction of the TWF characterized by converting a fraction of the heat extracted by cooling to useful mechanical work, which does not require external added heat and, therefore, is free of energy costs.
3. conversion of heat into useful mechanical work by the two above-mentioned methods with a fraction of the cooling heat recovered from the cooling process of the TWF (heat regeneration), which does not require heat and, therefore, is free of energy costs.
4. a convenient cascade coupling strategy of several power units characterized by taking advantage of the cooling heat from each previous power unit to power the next downstream power unit. A self-powered disruptive power plant can be achieved through the convenient combination of the four additive techniques conversion methods.

The result of the combination of the aforementioned methods is because while the amount of heat handled both in the form of heat addition and heat extraction is much higher than the useful work obtained, the net amount of external heat added is lower than the work useful obtained and consequently a thermal plant formed by several power units coupled in cascade is achieved, characterized by providing more useful work than the added external heat.

Therefore, it will now be introduced the thermal cycle responsible for carrying out the challenges posed: the VTVT thermal cycle is the isochoric-isothermal-isochoric-isothermal thermal cycle (R. Ferreiro Garcia et al. (2018) [22], and R. Ferreiro Garcia (2024) [23]. This cycle operates within the engine structure of a heat converter-based PU and is responsible for scheduling the thermodynamic transformations for doing useful work with strictly isothermal closed processes through both the expansion and contraction of the TWF. It operates with a vacuum when the atmospheric pressure is the reference pressure of the cycle. This means that the contraction-based useful work due to isochoric heat extraction is really performed by the vacuum and is achieved by cooling the TWF without state changes.

Implementing a PU responsible for converting heat into electrical power via useful mechanical work requires the arduous task of preliminary design to reduce as much error and deviation as possible from the expected results. Thus, a prototype can be developed that allows testing that requires the results to be adjusted based on the desired goals and proposed objectives. This PU must also be able to withstand a thermal cycle characterized by operating with closed adiabatic and strictly isothermal processes to obtain useful mechanical work for both the expansion and contraction of the TWF.

Each PU consists of two actuators based on RDACs that work intermittently; that is, when one of the actuator cylinders performs mechanical work due to the displacement of the piston, the other actuator cylinder remains at rest, and vice versa. This mode of operation is necessary because the isochoric processes of adding and removing heat do not allow the piston to move. Therefore, the time during which the piston of an actuating cylinder remains immobile is used to carry out isochoric processes. During that time, the second actuating cylinder also performs useful mechanical work.

Thomas Savery (1650–1715) [1], Thomas Newcomen (1664–1729) [2], and James Watt (1736–1819) [3] provided experimental evidence that doing work by vacuum-based contraction under closed processes due to cooling a TWF through heat extraction is associated with open-processes-based steam engines that were initially operated at atmospheric pressure through the thermal contraction (vacuum) of steam when it was condensed by cooling by heat extraction. Recently, J.G. van der Kooij (2015) [4], Alessandro Nuvolari (2004) [5]. Recently, Gerald Müller (2013) [6] presented an innovative concept concerning low-temperature-based atmospheric steam engines. Meanwhile, Gerald Müller and George Parker (2015) [7] conducted a series of experiments to assess this theory by including a forced expansion stroke at the location of the atmospheric steam engine; this implies that useful work is due to the presence of a vacuum was re-evaluated.

**2.1 RDAC structure as the basic component of PUs**

As depicted in Figure 1(a), a single RDAC actuator should be equipped with at least the following basic accessories:

1. a heat supply circuit comprising power sources, recirculation pumps, and heat supply transfer fluid (thermal oil and molten salt fluids)
2. a countercurrent heater (liquid/gas or gas/gas) to transfer heat from the heat transfer fluid to the hot side of the TWF
3. a hot TWF heated by forced convection by forced convection fans
4. a cold TWF circuit cooled by forced convection by forced convection fans
5. a countercurrent cooler (liquid/gas or gas/gas)
6. a heat extraction circuit comprising a heat sink, recirculation pump (not shown in the figures), and heat extraction transfer fluid (cool water or air)

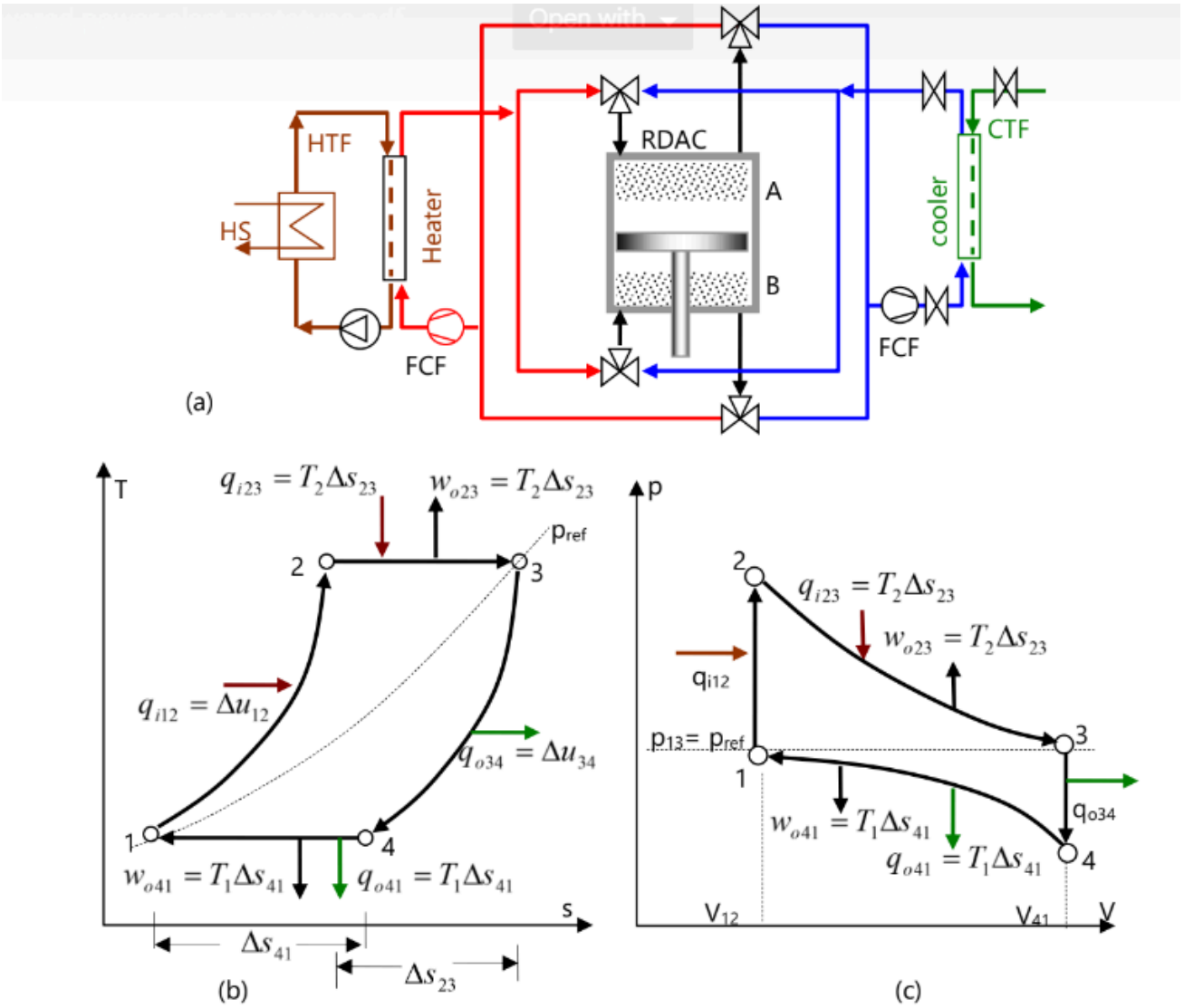


Figure 1: Simplified scheme of a discontinuous motion prototype of an RDAC necessary to implement a PU structure based on the patent application number: P202200035 and published number ES2956342A2 : (a) a semi-PU structure schematic without a heat recovery system at the cycle level for which every discontinuous motion type semi-PU is characterized by requiring double RDACs to complete a continuous motion cycle, (b) a T-s diagram of the non-regenerative VTVT thermal cycle executed in each cylinder chamber, and (c) a T-s diagram of the non-regenerative VTVT thermal cycle executed in each cylinder chamber.

Each RDAC is equipped with a volumetric clearance per cylinder chamber (A and B), which consists of a dead volume inside each cylinder chamber, which acts as a TWF reservoir. This structure is depicted in Figure 2. Continuous motion PUs comprising two discontinuous RDACs, each equipped with heat recovery systems (HRS), are also shown in the figure. Figure 2(a) depicts an HRS enabled to recover heat in parallel structure by independent HREx. Figure 2(b) depicts an HRS enabled to recover heat in parallel structure by a common HREx.

**2.2 Non-regenerative isochoric-isothermal-isochoric-isothermal (VTVT) thermal cycle**

Table 1 shows the cycle transformations presented in Equations (13)–(21) carried out in each cylinder chamber. The table also depicts the useful work, constant parameters, and heat transfer direction associated with each transformation.

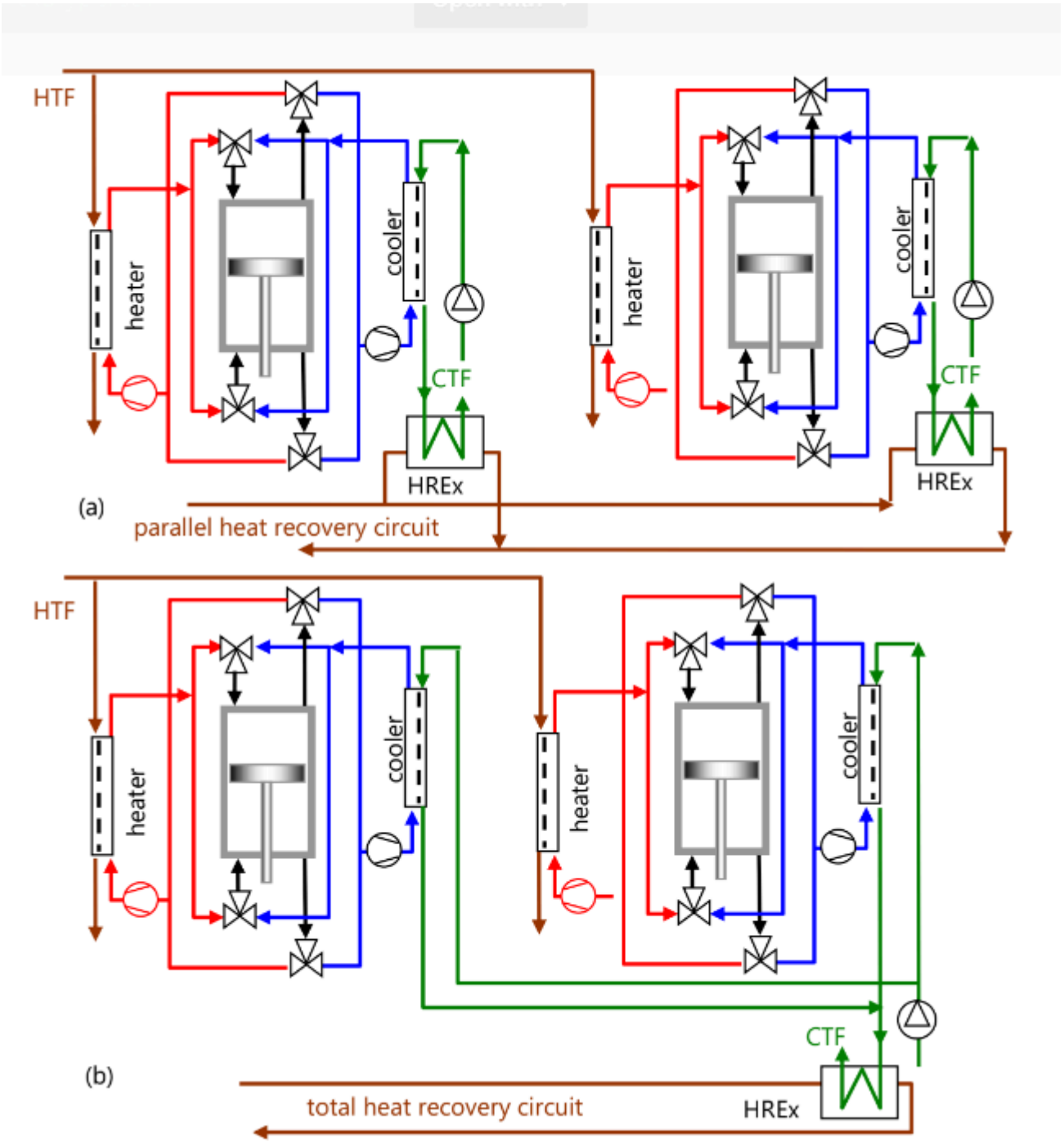


Figure 2: Depiction of continuous motion PUs comprising two discontinuous RDACs, each equipped with heat external heat recovery systems (HRSs): (a) an HRS enabled to recover heat in a parallel structure by an independent HREx and (b) an HRS enabled to recover heat in a parallel structure by a common HREx.

Figures 1(b) and 1(c) depict the T-s and p-V diagrams of the VTVT cycle and show the math models of the processes presented in Table 1. As shown in Figures 1(b) and (c), the transformations in the VTVT cycle are carried out in the following order: isochoric heat addition, isothermal expansion, isochoric heat extraction, and isothermal contraction.

Table 1: Cycle transformations carried out in the VTVT cycle showing the thermodynamic functions carried out simultaneously in both RDACs (A) and (B). The table also depicts the useful work, constant parameters and heat transfer direction associated with each transformation according to Equations (13-21)

| Cycle performed into cylinder chamber A | | | | Cycle performed into cylinder chamber B | | | |
|---|---|---|---|---|---|---|---|
| point | useful work | constant | heat in/out | point | useful work | constant | heat in/out |

| | | | | | | | |
|---|---|---|---|---|---|---|---|
| 1-2 | motion blocked | V | $q_{i12} = \Delta u_{12}$ | 3'-4' | motion blocked | V | $q_{o34} = \Delta u_{34}$ |
| 2-3 | $w_{o23} = T_2 \Delta s_{23}$ | T | $q_{i23} = T_2 \Delta s_{23}$ | 4'-1' | $w_{o41} = T_1 \Delta s_{41}$ | T | $q_{o41} = T_1 \Delta s_{41}$ |
| 3-4 | motion blocked | V | $q_{o34} = \Delta u_{34}$ | 1'-2' | motion blocked | V | $q_{i12} = \Delta u_{12}$ |
| 4-1 | $w_{o41} = T_1 \Delta s_{41}$ | T | $q_{o41} = T_1 \Delta s_{41}$ | 2'-3' | $w_{o23} = T_2 \Delta s_{23}$ | T | $q_{i23} = T_2 \Delta s_{23}$ |

The transformations carried out by the VTVT cycle in each RDAC chamber (A) and (B) are done sequentially in the following order: isochoric heat addition (V) constant in (1-2), isothermal expansion (T) constant doing useful work in (2-3), isochoric heat extraction (V) constant in (3-4), and isothermal contraction (T) constant doing useful contraction work in (4-1). Therefore, the VTVT thermal cycle proposed to operate in each RDAC (A) and (B) represented in Figure 1(a) is represented in Figure 1(b) and 1(c) and Table 1. This cycle comprises a sequence of four closed thermodynamic processes carried out along the proposed thermal cycle with a given TWF (in this case, helium and air) (E.W. Lemmon et al., 2007) [24].

As shown in Table 1, the first process is an isochoric heat addition process 1-2, during which the pressure, temperature, and entropy increase while the piston remains stationary. The second process is a closed process of isothermal expansion 2-3, which is responsible for doing output useful mechanical work. This requires the addition of an amount of heat equal to the work done. Since this process is not isochoric, the piston moves the entire stroke, while the pressure decreases as volume increases. The expansion process associated with the increase in entropy ends when the reference pressure at point 1 is reached at the end of the stroke.

The third process is an isochoric process of heat removal 3-4, during which the pressure, temperature, and entropy decrease while the piston remains stationary. Finally, the fourth process is a closed process of isothermal contraction 4-1, which causes the displacement of the piston throughout its stroke until the starting position at point 1. This process produces useful mechanical work, which decreases entropy and requires heat extraction equal to the work produced. The evolution in terms of the parameter's behavior of the VTVT cycle transformations is depicted in Table 2. The extraction of heat under an isothermal transformation responsible for the cooling of the TWF is carried out while obtaining useful mechanical work.

Based on the above description, the concept of obtaining useful work accompanied by a decrease in entropy (R. Ferreiro Garcia, 2023 [24]; R. Ferreiro Garcia, 2023) [25] for open processes-based cycles can be expressed by the following statement concerning isothermal vacuum-based work for closed processes: "The performance of mechanical work by closed process-based contraction due to a vacuum lead to a decrease in entropy." According to this statement, the decrease in entropy is a consequence of cooling only, regardless of temperature and pressure. The previous statement is shown in the transformation 4-1 in Table 2.

Experimental validation involves observing that no useful mechanical work is done if the vacuum is eliminated due to a lack of cooling in the condenser. This is because there is no difference in pressure between atmospheric and vacuum, causing the absence of forces between both sides of the piston. This idea is considered in this research work under closed processes to achieve mechanical work by strictly isothermal contraction under closed processes.

Table 2: Transformations carried out in each cylinder chamber of an RDAC operating in discontinuous mode with a VTVT cycle, showing the execution behavior in terms of *T*, *p*, *u*, and s changes for each cycle transformation carried out between any two transformations.

| $sp_i$-$sp_{(i+1)}$ | Closed cycle processes | Energy I/O | ΔT | Δp | Δv | Δu | Δs |
|---|---|---|---|---|---|---|---|
| 1-2 | isochoric heat addition | Heat in | + | + | = | + | + |
| 2-3 | strictly isothermal expansion | Work out | = | _ | + | = | + |
| 3-4 | isochoric heat extraction | Heat out | _ | _ | = | _ | _ |
| 4-1 | strictly isothermal contraction | Work out | = | + | _ | = | _ |

### 2.3 Thermodynamic properties of the VTVT cycle

The ideal thermal VTVT cycle depicted in Figures 1(b) and 1(c) exhibits certain thermodynamic properties for closed processes in terms of symmetries between changes in entropy, temperature, and internal energy in concordance with pressure and volume. Such properties follow both empirical and experimental observations. The characteristic of the ideal cycle implies the absolute absence of irreversibilities.

Therefore, assuming that

$$T_2 = T_3;\ \ T_1 = T_4\ , \tag{1}$$

undergoes the equalities of internal energy as

$$u_2 = u_3;\ \ u_1 = u_4\ . \tag{2}$$

Equation (2) has the following consequences:

$$T_2 - T_1 = T_3 - T_4 \tag{3}$$

Equations (2) and (3) have the following consequences such that it can be written as

$$\Delta T_{12} = \Delta T_{34} = \Delta T;\ \ \Delta u_{12} = \Delta u_{34} = \Delta u \tag{4}$$

Concerning entropy changes, it follows that

$$\Delta s_{23} = \Delta s_{41} = \Delta s \tag{5}$$

The equality defined in Equation (5) implies that

$$w_{o23} = T_2 \cdot \Delta s_{23} = T_2 \cdot \Delta s = q_{i23} \tag{6}$$

and

$$w_{o41} = T_1 \cdot \Delta s_{41} = T_1 \cdot \Delta s = q_{o41} \tag{7}$$

The combination of Equations (6) and (7) allows the following relationships to be modeled:

$$\begin{aligned} & w_{o41} / w_{o23} = T_1 \cdot \Delta s_{41} / T_2 \cdot \Delta s_{23} = \\ & = T_1 \cdot \Delta s / T_2 \cdot \Delta s = \\ & = T_1 / T_2 = \\ & = u_1 / u_2 = u_4 / u_3 \\ & = (p_1 . V_1) / (p_3 . V_3) = V_1 / V_3 \end{aligned} \tag{8}$$

It has been shown that the relationship between work, temperature, internal energy, heat transferred, and the consequent dependencies of pressure-volume-temperatures, regardless of the TWFs involved, according to Equation (8), exhibits the following behavior:

$$T_1 / T_2 = w_{o41} / w_{o23} = u_1 / u_2 = u_4 / u_3 = q_{o41} / q_{i23} = p_1 . V_1 / p_3 . V_3 = V_1 / V_3 \tag{9}$$

Equation (9) describes the ratio of isothermal temperatures (RIT) = $T_1/T_2$ in terms of work, internal energy, heat transferred, and pressure-volume ratios.

Equation (9) shows that the thermal efficiency increases if the ratio of work due to isothermal contraction and isothermal expansion (wo41/wo23) increases. This is because the heat that works by isothermal contraction is free of cost. This rigorous assertion leads to a theorem that will be stated below. This means that the higher the RIT, the higher the ratio between extracted to added heat $q_{i41}/q_{o23}$, which positively impacts thermal efficiency since the extracted heat has no cost ($q_{o41}$). This asseveration adheres to the fact that if the amount of extracted heat increases with respect to the amount of added heat, then the amount of contraction-based work increases with respect to the amount of work due to added heat.

On the basis of the observational evidence, the expressed idea can be mathematically described as

$$\underset{T2 \to T1}{Lim} \left| w_{41} / w_{23} \right) \right| = 1 \tag{10}$$

As a consequence of Equation (9), the ratio of heat transfer follows the same tendency such that

$$\underset{T2 \to T1}{Lim} \left| q_{41} / q_{23} \right| = 1 \tag{11}$$

The results of both limits imply that the maximum amount of heat extracted that can be converted to work is equal to the amount of heat added. This occurs when the high and low temperatures are equal. If both temperatures are equal, it is not possible to transfer heat, and thus, the meaning of Equations (10) and (11) is not achievable. As such, it will be necessary to find a compromise situation between the bottom $T_1$ and top $T_2$ values of the thermal cycle temperatures, such that the specific work and efficiency satisfy viable and acceptable performance criteria. Therefore, considering the ideal VTVT cycle, most of the relevant cycle characteristics from Equations (8)–(11) are governed by the following theorems:

**Theorem 1:** Theorem of the maximum value of the RIT

*The maximum value of the RIT is less than 1.*

Proof:

Theorem 1 establishes a maximum limit of possible values of the ratio of isothermal temperatures. The maximum value of the lower T of an ideal VTVT cycle (or $T_1$) cannot surpass the minimum value of the upper T or $T_2$. Therefore, $T_1 < T_2$, and, consequently, $(T_1/T_2) < 1$ or RIT < 1.

**Theorem 2:** Theorem of the functional efficiency dependence of the RIT

*If the ratio of the extracted to added heat ($q_{o41}/ q_{i23}$) increases in an ideal VTVT cycle, then the ratio of the vacuum-based work to the expansion-based work ($w_{o41}/w_{o23}$) increases.*

Since the RIT is a direct function of ($w_{o41}/w_{o23}$), efficiency is a direct function of RIT.

The theorem of functional efficiency dependence of the RIT, or $\eta_{th} = f(\text{RIT})$ and $\eta_{reg} = f(\text{RIT})$, states that the thermal efficiency increases as a function of the RIT.

Proof:

From the equalities shown in Equation (9), it follows that

$$RIT = T_1 / T_2 = w_{o41} / w_{o23} = q_{o41} / q_{i23} \tag{12a}$$

Equation (12a) can be represented as

$$w_{o41} / w_{o23} = q_{o41} / q_{i23} \tag{12b}$$

with Equation (12b) implying that

$$w_{o41} / q_{o41} = w_{o23} / q_{i23} \tag{12c}$$

where the left-hand side of Equation (12c) is

$$w_{o41} / q_{o41} = \eta_{th\_cont} \tag{12d}$$

which is the thermal efficiency of the useful contraction-based work ($w_{o\_cont}$) done by extracting heat by cooling the TWF without energy cost. The right part of Equation (12c) is

$$w_{o23} / q_{i23} = \eta_{th\_\exp} \tag{12e}$$

which is defined as the thermal efficiency of the expansion work ($w_{o\_exp}$) done by adding heat.

Therefore, when the ratio $w_{o41} / q_{o41} = \eta_{th\_cont}$ increases, the ratio $w_{o23} / q_{i23} = \eta_{th\_\exp}$ also increases. Consequently, the overall cycle efficiency which can be defined as

$$(w_{o23} + w_{o41}) / q_{i23} = \eta_{th} \tag{12f}$$

increases as a consequence. This conclusion confirms the established theorem.

The result of this consequence will be used to find a relationship between the RITs of working temperatures to give rise to exceptionally high efficiency at the expense of the specific work to achieve efficient self-powered PUs.

At these levels of description of the properties of the VTVT cycles, it can be asserted from Equations (1) and (12) that the ratio of the extracted heat to the added heat, which is equal to the ratio of the lower and upper temperatures of the thermal VTVT cycle, establishes the quality criterion of the cycle in terms of the self-feeding index (SFI) defined as

$$SFI = (\eta_{reg}\% - 100)/100 \quad (12g)$$

Starting with Equation (9), when the conditions to satisfy Equations (10) and (11) are met, the following relationship for the case of regenerative ideal VTVT cycles must also be met:

$$w_{o23} / q_{i23} = \eta_{reg} = 1 = 100\% \quad (12h)$$

and

$$(w_{o41}) / q_{i23} = \eta_{reg} = 1 = 100\% \quad (12i)$$

Consequently, Equation (12f) yields

$$(w_{o23} + w_{o41}) / q_{i23} = \eta_{reg} = 2 = 200\% \quad (12j)$$

Equation (12j) is a direct consequence of Equations (12h) and (12i). Thus, in an ideal VTVT cycle, the maximum achievable thermal efficiency is less than 200%. This leads to the proposal of Theorem 3 (the theorem of the limit of maximum SFI), which establishes that

**Theorem 3:** Theorem of the maximum value of the SFI

*The maximum achievable value of the SFI in an ideal VTVT cycle is unity or 100%.*

Proof:

Considering Equations (12h), (12i), and (12J), it follows that for a regenerative efficiency of 200% as per Equation (12J), the corresponding value of the SFI is 100% according to Equation (12g).

Some corollaries are derived as consequences of Theorem 3.

Corollary 1:

*The maximum achievable value of the regenerative efficiency in an ideal VTVT cycle is 2 or 200%.*

Corollary 2:

*The maximum achievable value of the SFI in any real VTVT cycle is less than 100%.*

**2.4 VTVT cycle transformations to operate an RDAC**

Figures 1(b) and (c) depict the T-s and p-V diagrams of the ideal VTVT cycle. The associated thermodynamic transformations described below are necessary to carry out a performance analysis.

Total added heat:

$$q_i = q_{i12} + q_{i23} = Cv \cdot (T_2 - T_1) + T_2 \cdot (s_3 - s_2) \quad (13)$$

According to Equations (4) and (13), this can be written as

$$q_i = \Delta u + T_2 \cdot \Delta s \quad (14)$$

Total extracted heat:

$$q_o = q_{o34} + q_{o41} = Cv \cdot (T_3 - T_4) + \cdot T_1 (s_4 - s_1) \quad (15)$$

According to Equations (4) and (15), this can be written as

$$q_o = \Delta u + T_1 \cdot \Delta s \quad (16)$$

The output work due to adding heat or heating responsible for expansion work ($w_{oexp}$) is

$$w_{o\exp} = w_{o23} = T_2 \cdot (s_3 - s_2) = T_2 \cdot \Delta s \quad (17)$$

The output work due to extracting heat or cooling responsible for contraction work ($w_{cont}$) is

$$w_{ocont} = \mid w_{o41} \mid = T_1 \cdot \mid (s_4 - s_1) \mid = T_1 \cdot \mid \Delta s \mid \quad (18)$$

The total output of useful work due to isothermal expansion and isothermal contraction is

$$w_o = w_n = w_{o23} + |\, w_{o41} \,| = T_2 \cdot (s_3 - s_2) + T_1 \cdot |\, (s_4 - s_1) \,| \tag{19}$$

which can be written as

$$w_o = w_n = T_2 \cdot \Delta s + T_1 \cdot |\, \Delta s \,| = (T_2 + T_1)\Delta s \tag{20}$$

since $|\, \Delta s \,| = \Delta s$

Thermal efficiency, which is the ratio of the output useful work to the total added heat, according to Equations (14) and (20), is

$$\eta_{th} = ratio\ (w_o / q_i) = \frac{(T_2 + T_1) \cdot \Delta s}{\Delta u + T_2 \cdot \Delta s} \tag{21}$$

Equation (21) is assimilated as the thermal efficiency for a non-regenerative thermal cycle that does useful mechanical work through closed and strictly isothermal processes.

**2.5 Controversial modeling inherent to contraction-based cycles, including the VTVT thermal cycle**

Part of the useful work of the cycle is due to the thermal contraction phase carried out by isothermal cooling, owing to the extraction of heat in a closed process. During this extraction process, useful mechanical work is done while entropy decreases. This phenomenon is responsible for the difference between energy balances. This thermal cycle exhibits contradictions in terms of the first principle concerning the energy balance (heat and work) carried out in conventional thermal cycles, which do output mechanical work only by adding heat. This is because it is possible to do useful mechanical work via the thermal contraction of a working thermal fluid by extracting heat. Therefore, according to Equations (13) and (14), the added heat is

$$q_i = \Delta u + T_2 \cdot \Delta s = \Delta u + w_{o\exp} \tag{22}$$

Furthermore, according to Equations (15) and (16), the extracted heat is

$$q_o = \Delta u + T_1 \cdot \Delta s = \Delta u + w_{ocont} \tag{23}$$

From Equation (20), the net output useful work is

$$w_o = w_n = T_2 \cdot \Delta s + T_1 \cdot |\, \Delta s \,| = (T_2 + T_1)\Delta s = w_{o\exp} + w_{ocont} \tag{24}$$

The energy balance of a conventional thermal cycle satisfies the following equation:

$$q_i - q_o = w_o = w_n \tag{25}$$

Implementing Equations (22) and (23) into Equation (25) yields

$$q_i - q_o = w_o = \Delta u + w_{o\exp} - (\Delta u + w_{ocont}) = w_{o\exp} - w_{ocont} \tag{26}$$

Equation (26) yields a different result than Equation (25). This difference indicates a discrepancy between the energy balances of conventional thermal cycles and thermal cycles based on thermal contraction. In addition, no fundamental laws of thermodynamics are violated when modeling energy balances based on the first principle. We considered the steam engines that operated at atmospheric pressure on the high-pressure side and a vacuum at the low-pressure side caused by the condensation of steam at a constant temperature [4–9], where useful mechanical work is done undergoing an isothermal decrease in entropy. This controversy has been assiduously accepted for more than two centuries, for example, by Newcomen (1664–1729) [4] and James Watt (1736–1819) [5]. Based on this controversy, RDACs operating at atmospheric pressure on the side of high pressure and in a vacuum on the side of low pressure have been used.

Consequently, the differences between output mechanical work $w_o$ definitions for thermal cycles that operate by expansion or expansion plus contraction are described below.

Thermal cycles that do work by expansion (conventional thermal cycles operating with open or closed processes):

$$w_o = q_i - q_o = w_{o\exp} \tag{27}$$

Thermal cycles that do work by expansion and contraction (based on RDACs operating with closed processes):

$$w_o = w_{o\exp} + w_{ocont} \tag{28}$$

### 2.6 Regenerative VTVT cycle

Throughout this article, two heat regeneration strategies will be analyzed by applying internal heat recovery strategies. These consist of the following:

-- use the heat transferred to the thermal cooling fluid by transfer to the same cycle in its same PU

-- use the heat transferred to the thermal fluid for cooling transfer to other downstream PUs

Figures 2, 3, and 4 show that a significant fraction of the heat extracted to generate the vacuum and work by the thermal contraction of the TWF in the discontinuous thermal cycle described above can be recovered and used by a heat regeneration strategy in the considered thermal cycle depicted in Figures 6(a) and 6(b). The final temperature of the expansion process is equal to the initial temperature, which means that the final internal energy is equal to the initial internal energy. At the final stage of the expansion process, this significant amount of heat is transferred to the cooling fluid as extracted heat using a recovery technique described by Ramon Ferreiro (2023) [24]–[25]. Consequently, the cooling fluid contains a useful fraction of the transferred heat in the form of low-grade heat. The heat regeneration process aims to recover as much of this transferred heat as possible.

According to the T-s and p-V diagrams in Figures 3(a) and 3(b), the heat regeneration procedure is modeled as follows:

$$q_{i12} = q_{iext} + q_{reg34} \tag{29}$$

The heat recovery factor is the ratio of the amount of heat regenerated ($q_{reg34}$) to the amount of heat extracted ($q_{o34}$) by cooling and is calculated as

$$RF = \frac{q_{reg34}}{q_{o34}} \tag{30}$$

$$q_{reg34} = RF \cdot q_{o34} \tag{31}$$

The external heat added to the cycle is achieved by combining Equations (14) and (15), which yields

$$q_{iext} = q_{i12} - q_{reg34} = q_{i12} - RF \cdot q_{o34} \tag{32}$$

Equation (31) shows that the higher the heat recovery ($q_{reg34}$), the lower the amount of external heat ($q_{iext}$) added to the cycle. This increases the ratio of the net work to the external heat added and, consequently, the thermal efficiency of the cycle.

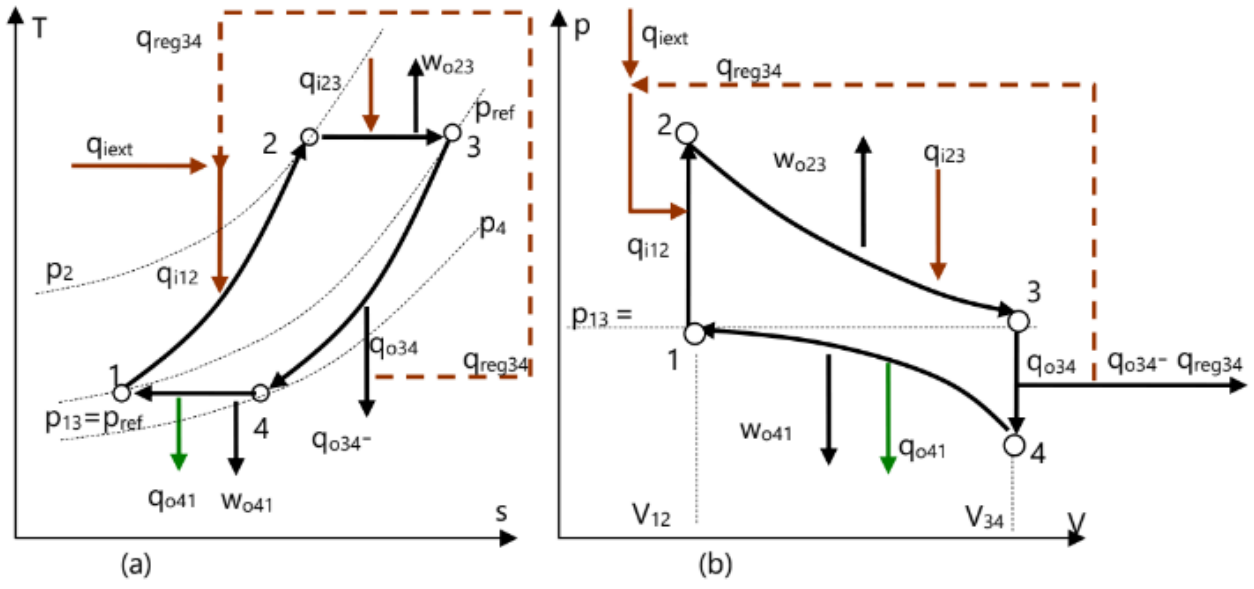

Figure 3: Internally regenerative VTVT thermal cycles depicting the thermodynamic processes carried out during each regenerative cycle: (a) a T-s regenerative diagram and (b) a p-V regenerative diagram.

**2.7 Modeling performance criteria**

In conventional thermal cycle analyses (for thermal cycles in which the useful work is due only to the addition of heat), the relationship between thermodynamic work and added heat is considered a performance criterion; meanwhile, all types of energy losses (thermal efficiency) are neglected. In the case under study, there are other behavioral indices, including those described below.

The ratio of the work achieved by heat extraction to the work achieved by total heat addition is given as

Ratio $\frac{w_{ocont}}{w_{o\exp}}$. (33)

The thermal efficiency of the ratio of the work achieved by adding heat to the added heat (isochoric plus isothermal) is given as

$$\eta_{\text{th\_exp}} = \frac{w_{o\exp}}{q_i} = \frac{w_{o\exp}}{q_{i12} + q_{i23}}. \quad (34)$$

The thermal efficiency of the work achieved by heat extraction to the extracted heat (isochoric plus isothermal) is given as

$$\eta_{\text{th\_cont}} = \frac{w_{ocont}}{q_o} = \frac{w_{ocont}}{q_{o34} + q_{o41}}. \quad (35)$$

Thermal efficiency, as the ratio of the net work due to heat addition to the total added heat (isochoric plus isothermal), is given as

$$\eta_{th} = \frac{w_n}{q_i} = \frac{w_{o\exp} + w_{ocont}}{q_{iext} + q_{i23}}. \quad (36)$$

According to Equation (36), $q_{iext} = q_{i12} - q_{reg34}$, where $q_{reg34} = 0$ for a cycle without heat regeneration. Thus, $q_{iext} = q_{i12}$. Consequently, Equation (31) can be written as

$$\eta_{th} = \frac{w_n}{q_i} = \frac{w_{o\exp} + w_{ocont}}{q_{i12} + q_{i23}}. \quad (37)$$

The regenerative cycle thermal efficiency is defined as the ratio of net work (due to the external heat added plus the heat extracted) to the added external heat and is given as

$$\eta_{th\_reg} = \frac{w_n}{q_i} = \frac{w_{o\exp} + w_{ocont}}{q_{iext} + q_{i23}} = \frac{w_{o\exp} + w_{ocont}}{q_{i12} - q_{reg34} + q_{i23}} = \frac{w_{o\exp} + w_{ocont}}{q_{i12} - RF \cdot q_{o34} + q_{i23}}. \quad (38)$$

Equation (36) exhibits disruptive consequences for the thermal cycle that need to be further explained. Useful work is done by contracting the TWF as a consequence of the heat extracted by cooling the confined working fluid into a cylinder chamber. Useful work is also done by regenerating the heat recovered from the extracted heat. Therefore, a high value of the heat recovery factor combined with a low irreversibility factor (including thermal and mechanical irreversibility) can cause the useful work output to be greater than the external heat input. In this case, the PU can produce useful work without adding external heat to the thermal cycle. This makes it possible to feed the PU back from the output power via electrical heating and to take advantage of the excess power produced without needing to provide heat from an external source. This issue is addressed in the analysis of the results to estimate the achieved auto-power based on PU irreversibility and regenerated heat.

**2.8 The performance of the ideal case for a regenerative VTVT cycle**

In the ideal case, losses are neglected. Thus, LF = heat recovery factor = 1, and RIT approaches 1. This means that thermal and mechanical losses are neglected and the heat recovery system effectiveness approaches 100% subject to an RIT that approaches unity.

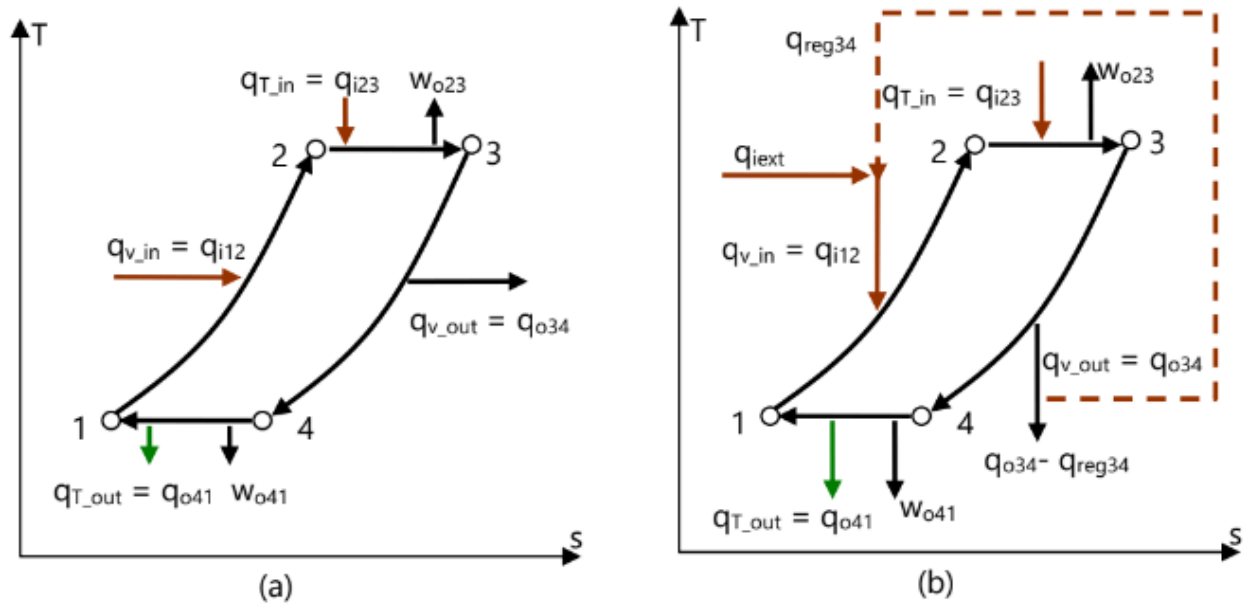


Figure 4: T-s diagram of an ideal regenerative VTVT cycle: (a) a non-regenerative cycle and (b) a regenerative cycle.

The notation used in the energy balance of the ideal regenerative VTVT cycle according to the first law is described as

- isochoric heat transfer inlet, denoted as $q_{v\_in} = q_{i12}$
- isochoric heat transfer outlet, denoted as $q_{v\_out} = q_{o34}$
- isothermal heat transfer inlet, denoted as $q_{T\_in} = q_{i23} = w_{o23}$
- isothermal heat transfer outlet, denoted as $q_{T\_out} = q_{o41} = w_{o41}$

The ideal balance according to the diagram depicted in Figure 4(a) is as follows:

$$q_{v\_in} - q_{v\_out} = 0, \; or \; q_{i12} - q_{o34} = 0 \tag{39}$$

$$q_{T\_in} - w_{o23} = 0 \; or \; q_{i23} - w_{o23} = 0 \tag{40}$$

$$q_{T\_out} - |\, w_{o41} \,| = 0 \;\; or \; q_{o41} - |\, w_{o41} \,| = 0 \tag{41}$$

On the basis of energy balance, Equation (39) indicates that the amounts of isochoric added and isochoric extracted heat are equal. Thus, if the amount of isochoric extracted heat $q_{o34}$ could be ideally 100% recovered, no losses would be assumed in the isochoric heat energy balance. Equation (40) indicates that the amount of isothermal heat added along the process 2-3 is ideally 100% converted to work $w_{o23}$ at the cost of the added heat $q_{s\_in} = q_{i23}$. Therefore, the work done in Equation (41) ideally does not consume added heat but is free work. Consequently, if the heat recovery factor (RF) is 1, the other thermal and mechanical irreversibilities defined as losses factor (LF) are also 1 (or LF=1), and the RIT approaches unity, then the amount of free net work achieved approaches the amount of isothermal extracted heat, which approaches the amount of isothermal added heat as stated by Equations (7-9). That is, from Equation (41), it follows that

$$q_{T\_out} = |\, w_{o41} \,| \;\; or \; q_{o41} = |\, w_{o41} \,| \tag{42}$$

Equation (42) indicates that 100% of the amount of isothermal extracted heat is converted into mechanical work at no cost. Then, considering the ideal case for which the losses factor and the heat recovery factor approach unity (LF=RF=1), the cost-free energy obtained is close to the added input heat. In summary, the heat added during isothermal expansion $q_{i23}$ is compensated by the work produced $w_{o23}$, and the heat added during isochoric heat addition $q_{i12}$ is compensated by the recovered and regenerated heat $q_{o41}$. Meanwhile, the heat extracted at zero cost during isothermal contraction $q_{o41}$ is converted into useful work at no cost. In a real cycle, inherent losses must be taken into account so that the benefits derived from the absence of losses cannot be achieved in concordance with the second law.

Figure 4(b) depicts a heat recovery circuit applied on a T-s diagram of a VTVT cycle. In such a heat recovery structure, the maximum possible amount of heat recovered (the ideal case) will approach only 50% of the available heat $q_{o34}$. The proposed case studies will consider approaches to viable, realistic cases.

**3 Case studies related to cascaded power units to achieve self-feed power plants**

In the presented case study, an attempt is made to explore the multidimensional space of results potentially susceptible to being subjected to experimental testing based on criteria of efficiency and specific work. After being described and analyzed, the disruptive thermal power plant to be prototyped is simulated. Its results are then discussed to make the appropriate adjustments prior to physical prototyping. The thermodynamic model of a single RDAC that is depicted in Figure 1(a) and described by Equations (13)–(21) and whose T-s and p-V diagrams are represented in Figure 1(b) and (c) are used to carry out a set of case studies on a cascaded coupled set of PUs. This is done while considering the specific work and thermal efficiency as a function of the ratio of bottom to top temperatures (RIT), the losses factor (LF), and the heat recovery factor (HRF), represented as

$$w_o = f_w(RIT, p_{ref}, LF, RF) \tag{43}$$

$$\eta_{th} = f_\eta(RIT, p_{ref}, LF, RF) \tag{44}$$

or, in the case of heat regeneration,

$$\eta_{reg} = f_{\eta reg}(RIT, p_{ref}, LF, RF) \tag{45}$$

The next task consists of achieving desired performance results from cycle analyses that express the work done by the isothermal expansion and isothermal contraction for a discontinuous motion prototype depicted in the T-s and p-V diagrams in Figure 2, as well as performance parameters useful for evaluating the achievements concerning to the proposed thermal engines in which two discontinuous RDACs are needed to complete a single continuous motion PU. The prototype based on the set of two discontinuous motion RDACs depicted in Figure 1(a) is critical for implementing a complete regenerative power plant characterized by a cascade of PUs regardless of whether they are regenerative.

The cycle represented in Figures 1(a), 1(b), 2(a), and 2(b) was calculated for a group of cases arranged as a function of top temperatures ranging from 400 K to 800 K, as depicted on Table 3, using helium as a real working fluid (Lemmon E.W. et al., 2007) [24].

The input data required for the VTVT thermal cycle analysis consists of the state point temperatures *T*[K], pressures p[bar], specific volume *v*[kJ.kg$^{-1}$], specific internal energy *u*[kJ.kg$^{-1}$], and specific entropy *s*[kJ.kg$^{-1}$.K].

In Case Study 1 in Table 3, the top temperature fixed at 800 K requires a bottom cycle temperature of 792 K to achieve an RIT of 0.99. The values of specific volume, internal energy, and specific entropy of 8.17430 [kJ.kg$^{-1}$], 2472.90 [kJ.kg$^{-1}$], and 31.595 [kJ.kg$^{-1}$.K], respectively, are obtained using the standard database of Lemmon E.W. et al. (2007) [24] for helium as the working fluid and considering SP 1, with a temperature of 792 K, and a pressure of 1 bar (the atmospheric reference pressure).

Since the change from SP 1 to SP 2 consists of a closed isochoric heat addition process, the volume remains constant at 8.17430 [kJ.kg$^{-1}$], while the temperature increases to 800 K. Therefore, the corresponding pressure, internal energy, and entropy are achieved by entering such parameters (isochoric volume and temperature).

The change from SP 2 to SP 3 consists of a closed isothermal heat addition process at 800 K associated with a simultaneous conversion heat-to-work expansion process, which ends at the initial pressure of 1 [bar], and the associated values of the specific volume, internal energy, and specific entropy are 8.25690 [kJ.kg$^{-1}$], 2497.90 [kJ.kg$^{-1}$], and 31.648 [kJ.kg$^{-1}$.K], respectively.

For the next SP change, since the change from SP 3 to SP 4 consists of a closed isochoric heat extraction process, the volume remains constant at 8.25690 [kJ.kg$^{-1}$], while the temperature decreases to 792 K. Therefore, the corresponding pressure, internal energy, and entropy of 0.9798 [bar], 2472.90 [kJ.kg$^{-1}$], and 31.616[kJ.kg$^{-1}$.K], respectively, are achieved by entering such parameters (isochoric volume and temperature). Note that the actual pressure is a vacuum of 0.9798-1 = 0.0211[bar]. Finally, the change from SP 4 to SP 1 (the initial cycle conditions) consists of a closed isothermal heat extraction process at 972 [K] associated with a simultaneous conversion heat-to-work contraction process, which ends at the initial pressure of 1 [bar]. The initial associated values of the specific volume, internal energy, and specific entropy correspond to SP 1. The rest of the study cases are processed following the same methodology by simply assigning the corresponding RIT.

Table 3: Data resulting from ideal VTVT cycle computation of six cases with helium as the working fluid corresponding to the T-s and p-V diagrams depicted in Figures 1(b), 1(c), and 3 for regenerative cycles.

| Case study 1: RIT = 0.99 | | | | | |
|---|---|---|---|---|---|
| SPs | *T*[K] | p[bar] | *v*[kJ.kg$^{-1}$] | *u*[kJ.kg$^{-1}$] | *s*[kJ.kg$^{-1}$.K] |
| 1 | 792.00 | 1 | 8.17430 | 2472.90 | 31.595 |
| 2 | 800.00 | 1.0203 | 8.17430 | 2497.90 | 31.627 |
| 3 | 800.00 | 1 | 8.25690 | 2497.90 | 31.648 |
| 4 | 792.00 | 0.9798 | 8.25690 | 2472.90 | 31.616 |
| Case study 2: RIT = 0.98 | | | | | |
| 1 | 784.00 | 1 | 8.09180 | 2448.00 | 31.543 |
| 2 | 800.00 | 1.0411 | 8.09180 | 2497.90 | 31.606 |
| 3 | 800.00 | 1 | 8.25690 | 2497.90 | 31.648 |
| 4 | 784.00 | 0.9597 | 8.25690 | 2448.00 | 31.585 |
| Case study 3: RIT = 0.95 | | | | | |
| 1 | 760.00 | 1 | 7.84420 | 2373.20 | 31.381 |
| 2 | 800.00 | 1.1060 | 7.84420 | 2497.90 | 31.541 |
| 3 | 800.00 | 1 | 8.25690 | 2497.90 | 31.648 |
| 4 | 760.00 | 0.8993 | 8.25690 | 2373.20 | 31.488 |
| Case study 4: RIT = 0.9 | | | | | |
| 1 | 720.00 | 1 | 7.43150 | 2248.60 | 31.100 |
| 2 | 800.00 | 1.2000 | 7.43150 | 2497.90 | 31.429 |
| 3 | 800.00 | 1 | 8.25690 | 2497.90 | 31.648 |
| 4 | 720.00 | 0.7987 | 8.25690 | 2248.60 | 31.319 |
| Case study 5: RIT = 0.7 | | | | | |
| 1 | 560.00 | 1 | 5.78080 | 1750.00 | 29.795 |
| 2 | 800.00 | 1.8627 | 5.78080 | 2497.90 | 30.907 |
| 3 | 800.00 | 1 | 8.25690 | 2497.90 | 31.648 |
| 4 | 560.00 | 0.3961 | 8.25690 | 1750.00 | 30.536 |
| Case study 6: RIT = 0.5 | | | | | |
| 1 | 400.00 | 1 | 4.13000 | 1251.50 | 28.048 |
| 2 | 800.00 | 3.0130 | 4.13000 | 2498.00 | 30.208 |
| 3 | 800.00 | 1 | 8.25690 | 2597.90 | 31.648 |
| 4 | 400.00 | 0.000 | 8.25690 | 1251.50 | 29.488 |

### 3.1 Relevant results of an ideal regenerative VTVT cycle as a function of design variable parameters

Through Equations (1)–(12), preliminary design criteria have been established through which the strategy aimed at searching for design results of a disruptive prototype enabled to achieve sustainable self-feeding is facilitated. According to Figure 5, the data represented in Table 3 are obtained from a set of input causal variables, such as high and low operating temperatures (TH), TL, a reference pressure $p_{ref}$, a proposed RIT, a regenerative factor (RF), and a losses factor (LF). Consequently, the results of Table 4 are achieved by conveniently processing the data in Table 3, including net work $w_n$, thermal efficiency $\eta_{th}$, regenerative thermal efficiency $\eta_{th\_reg}$, and the SFI.

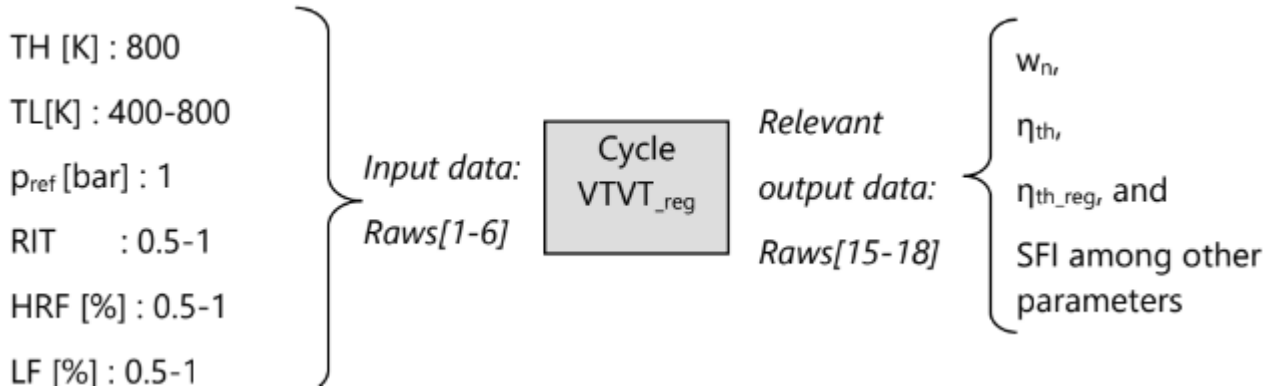


Figure 5: Structure of the causal relevant input/output variable parameters in the analysis of the regenerative VTVT cycle. The results of the processed data according to the scheme of Figure 5 (shown in Table 3) are depicted in Table 4.

Table 4 depicts the data resulting from the ideal VTVT cycle analysis depicted in Table 3. The results are organized according to the structure shown in Figure 5. The results presented in Table 4 cannot be achieved in real experiments since no losses have been considered. Therefore, the results shown in Table 4 are intended to serve as a guide for the design of prototypes in establishing useful design criteria. Furthermore, such results make it possible to judge the validity of the proposed input data based on the output results that best adapt to the expectations of the prototype performance to be implemented. The energy balance based on the first law depicted in Figure 4 and Equations (39)–(42) is considered the ideal study.

Table 4: Results of the case studies considered in Table 3 in terms of performance as a function of the RIT for a series of six ideal cases characterized by the absence of irreversibilities subjected to the highest and unachievable RIT according to the constraints imposed by the second law.

| I/O | Row | Test | 1 | 2 | 3 | 4 | 5 | 6 |
|---|---|---|---|---|---|---|---|---|
| Input data | 1 | TH [K] | 800.00 | 800.00 | 800.00 | 800.00 | 800.00 | 800.00 |
| | 2 | TL [K] | 792.00 | 784.00 | 760.00 | 720.00 | 560.00 | 400.00 |
| | 3 | RIT*100 | 99.00 | 98.00 | 95.00 | 90.00 | 70.00 | 50.00 |
| | 4 | LF | 1 | 1 | 1 | 1 | 1 | 1 |
| | 5 | RF | 1 | 1 | 1 | 1 | 1 | 1 |
| | 6 | $p_{ref}$ [bar] | 1 | 1 | 1 | 1 | 1 | 1 |
| Output data | 7 | $q_{i\_12+23}$ [kJ.kg$^{-1}$] | 41.80 | 83.50 | 210.30 | 424.50 | 1340.70 | 2398.50 |
| | 8 | $q_{i\_ext}$ [kJ.kg$^{-1}$] | 16.80 | 33.60 | 85.60 | 175.20 | 592.80 | 1052.10 |
| | 9 | $q_{o\_34+41}$ [kJ.kg$^{-1}$] | 41.63 | 82.83 | 206.02 | 406.98 | 1162.86 | 1922.40 |
| | 10 | $w_{o23}$ [kJ.kg$^{-1}$] | 16.80 | 33.60 | 85.60 | 175.20 | 592.80 | 1152.00 |
| | 11 | $w_{o41}$ [kJ.kg$^{-1}$] | 16.63 | 32.93 | 81.32 | 157.68 | 414.96 | 576.00 |
| | 12 | $\eta_{\_exp}$ [%] | 40.19 | 40.24 | 40.70 | 41.27 | 44.22 | 48.03 |
| | 13 | $\eta_{\_cont}$ [%] | 39.95 | 39.75 | 39.47 | 38.74 | 35.68 | 29.96 |
| | 14 | TH-TL | 8.00 | 16.00 | 40.00 | 80.00 | 240.00 | 400.00 |
| | 15 | $w_n$ [kJ.kg$^{-1}$] | 33.43 | 66.53 | 166.92 | 332.88 | 1007.76 | 1728.00 |
| | 16 | $\eta_{\_reg}$ [%] | 199.00 | 198.00 | 195.00 | 190.00 | 170.00 | 164.24 |
| | 17 | $\eta_{\_th}$ [%] | 79.98 | 79.67 | 79.37 | 78.42 | 75.17 | 72.05 |
| | 18 | SFI | 99.00 | 98.00 | 95.00 | 90.00 | 70.00 | 64.24 |

The exploration of the behavior of the regenerative VTVT disruptive cycle for different RIT values provides outstanding conclusions that lead to completely unsuspected design criteria in terms of efficiency, as shown in Table 4.

Given the variation of the RIT from an approach to its maximum value (0.99) to an arbitrary low value (0.5), the reversible cycle behavior exhibits interesting trends. Thus, the most relevant changes responsible for indicting interesting trends follow the RIT according to the following results:

-- Isothermal work done by expansion increases as the RIT increases (row 10).

-- Isothermal work done by contraction increases as RIT decreases (row 11).

-- Thermal efficiency due to expansion increases as RIT decreases (row 12).

-- Thermal efficiency due to contraction decreases as the RIT decreases (row 13).

-- Heat added to the cycle increases as RIT decreases (row 7).

-- Net work increases as RIT decreases (row 15).

-- Thermal efficiency with regeneration decreases as the RIT decreases (row 16).

-- Thermal efficiency without regeneration decreases as RIT decreases (row 16).

-- Self-feed index SFI decreases as the RIT decreases (row 18)

In summary, the ideal regenerative VTVT cycle operating under ideal conditions provides results that clearly mark the lines of advance in heat-work conversion techniques to achieve highly efficient self-powered machines.

**3.2 Self-powered power plant based on irreversible internally regenerative PUs coupled in cascade using helium or air as the working fluid**

As depicted in Figure 6, the internal heat recovery and regeneration system operates by mixing the hot working fluid after expansion in chamber A and the cold working fluid before expansion in chamber B. This is done in such a way that the amount of heat transferred when the temperature of both chambers A and B is in thermal equilibrium, it is equivalent to half of the heat available in either chamber after an isothermal expansion. Therefore, the maximum amount of heat recoverable through mixing the working fluids into both chambers is 50% of the available heat. Thus, the RF is assumed to be 0.5 or 50%.

The remainder of the unrecovered heat can be recovered and partially regenerated from the thermal cooling fluid. Consequently, the internal regeneration strategy could be enhanced by recovering the useful heat rejected to the cooling system, which will contribute to increasing the amount of net useful work without adding external heat, thus increasing the efficiency and the SFI.

The study of cases is proposed considering irreversibilities both in terms of mechanical and thermal losses and the losses inherent to heat recovery strategies to reinforce the study on realistic (non-ideal) cases. Thus, the next study deals with internally and externally regenerative irreversible VTVT cycles. It is assumed that a maximum of only 50% of the available heat could be recovered in the case of an internal regenerative cycle. Meanwhile, for external regenerative cycles, it is supposed a priori that up to 90% of the available heat could be recovered using state-of-the-art technology in countercurrent heat transfer techniques.

Figure 6 depicts the internal heat recovery structure and the foundation of the internal heat regeneration strategy. Figures 6(a) and 6(b) show the changes in temperatures in cylinder chambers A and B for both cases (at the end of each stroke) when the movement of the cylinder piston remains blocked to achieve isochoric heat transfer processes. The heat of a cylinder chamber that is initially at a higher pressure is transferred to the cylinder chamber that is initially at a lower temperature. This transfer process ends when thermodynamic equilibrium is reached (equal temperatures in both chambers). Thus, 50% of the heat in the cylinder chamber with the higher temperature is transferred to the cylinder chamber with the lower temperature. This heat transfer system is based on thermal balance or the mixture of energies and masses in forced thermal convection. This concept is depicted in Figure 6(c), where the basic heat recovery circuit is depicted by dashed lines and no heat transfer control valves are shown. The symbol assigned to each PU and depicted in Figure 6(c) is used to manage more complex schemes.

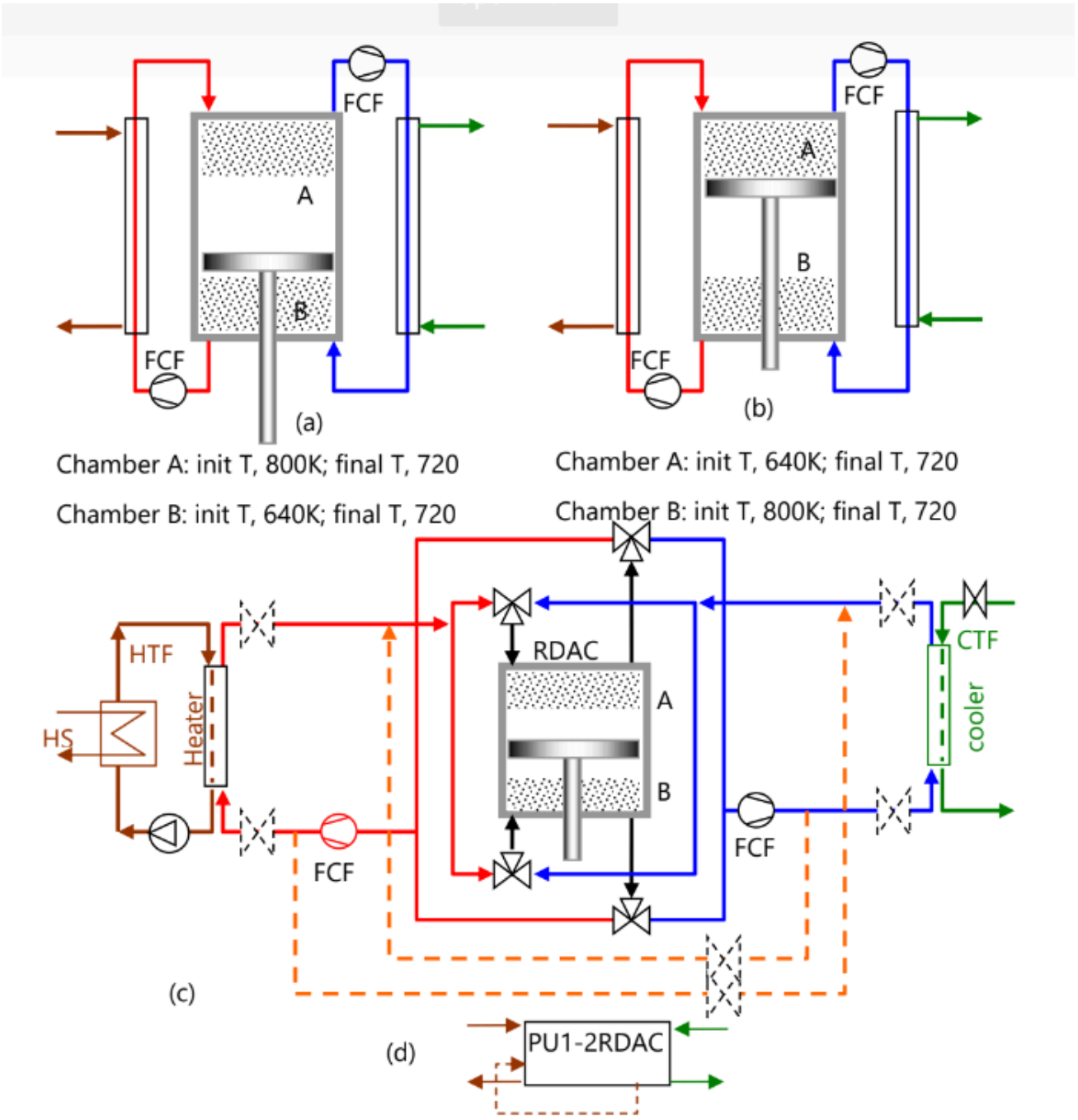


Figure 6: Internal heat recovery structures and the foundation of internal heat regeneration strategy according to the patent application No. 2202000035: (a) chamber A (cooling) and chamber B (heating), (b) chamber A (heating) and chamber B (cooling), (c) schematic representation of an internally regenerative RDAC, and (d) symbolic representation of an internally regenerative PU composed by two discontinuous internally regenerative RDACs to achieve a continuous output motion PU.

The general schemes of the cascaded VTVT-based PPs are depicted in Figure 7. I/O temperatures, RIT, LF, and RF are similar for each PU of helium- and air-based cascaded PPs. The study of cases is proposed considering irreversibilities both in terms of mechanical and thermal losses and the losses inherent to heat recovery strategies to reinforce the study on realistic (non-ideal) cases. Thus, the next study deals with internally and externally regenerative VTVT irreversible cycles. It is assumed a priori that up to 90% of the available heat could be recovered using state-of-the-art technology in countercurrent heat transfer techniques, according to Meeta Sharma et al. (2014) [20] and Meeta Sharma et al. (2016) [21].

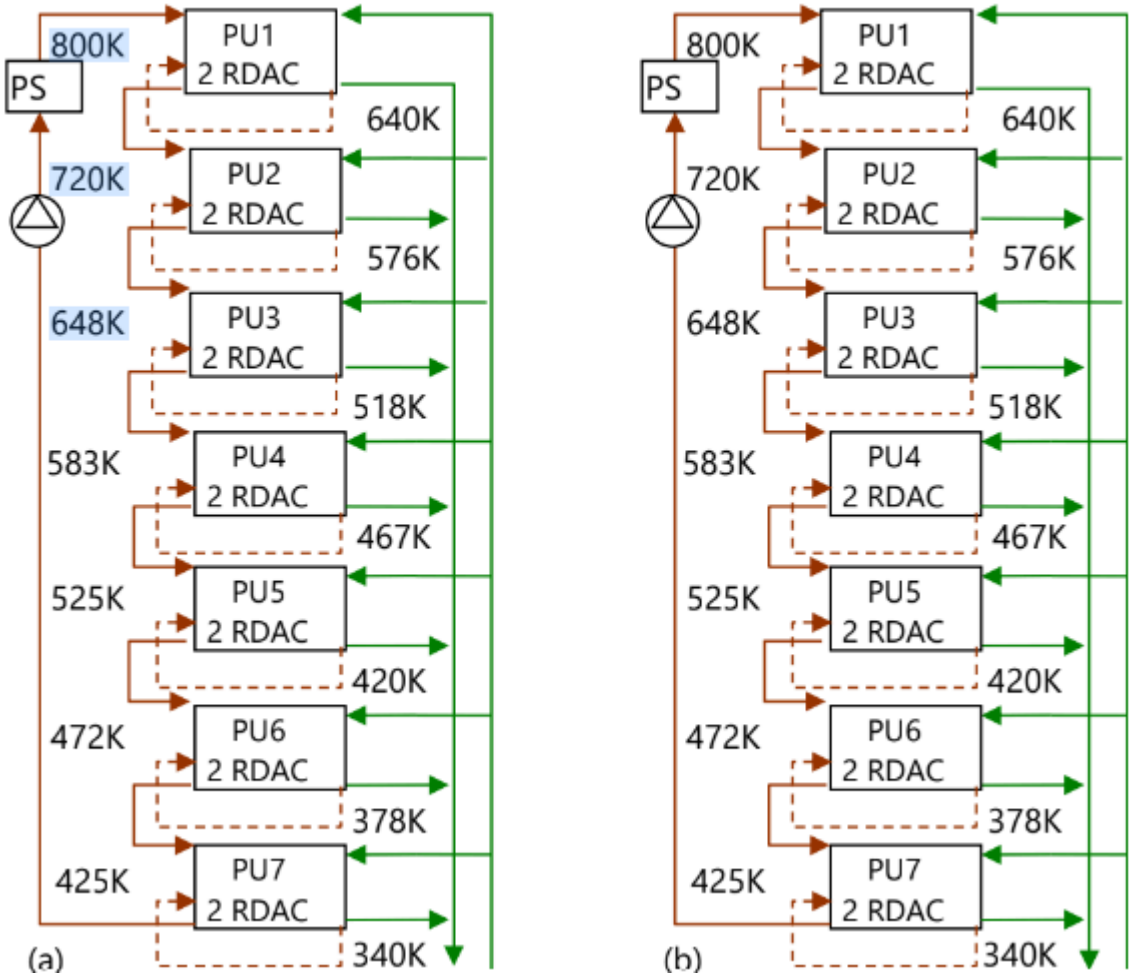


Figure 7: Case study of an internally irreversible regenerative VTVT cycle consisting of seven cascaded PUs, with (a) helium as the working fluid and (b) air as the working fluid. Although the I/O temperatures of each PU are equal for both PPs (PP(a) with He and PP(b) with Air), most of the common parameters, including efficiency and SFI, are different.

Table 5 depicts the data obtained from the irreversible VTVT cycle analysis for a PP consisting of seven PUs with internal heat regeneration connected in the cascade depicted in Figure 7(a). Given that more than half of the heat rejected by the VTVT cycle cannot be recovered, it remains in the thermal cooling fluid. It could subsequently be used through a feeding system for another cascade of PUs, which would significantly increase the regenerative efficiency of the power plant. This case study is not considered in this work.

Table 5: Data resulting from the irreversible VTVT cycle analysis for a PP consisting of seven PUs with internal heat regeneration connected in cascade. The analysis is focused on the SFI as a function of the RIT, assuming an internal heat regeneration factor of 0.5 = 50%, a losses factor of LF = 0.9, and the use of real helium as the working fluid.

| PU 1 | | | | | |
|---|---|---|---|---|---|
| SPs | $T$[K] | p[bar] | $v$[kJ.kg$^{-1}$] | $u$[kJ.kg$^{-1}$] | $s$[kJ.kg$^{-1}$.K] |
| 1 | 640.00 | 1 | 6.60610 | 1999.30 | 30.489 |
| 2 | 800.00 | 1.5033 | 6.60610 | 2497.90 | 31.184 |
| 3 | 800.00 | 1 | 8.25690 | 2497.90 | 31.648 |
| 4 | 640.00 | 0.5974 | 8.25690 | 1999.30 | 30.952 |
| PU 2 | | | | | |
| 1 | 576.00 | 1 | 5.94580 | 1799.90 | 29.942 |

| | | | | | |
|---|---|---|---|---|---|
| 2 | 720.00 | 1.5033 | 5.94580 | 2248.60 | 30.637 |
| 3 | 720.00 | 1 | 7.43150 | 2248.60 | 31.100 |
| 4 | 576.00 | 0.5974 | 7.43150 | 1799.90 | 30.405 |
| PU 3 | | | | | |
| 1 | 518.40 | 1 | 5.35160 | 1620.40 | 29.394 |
| 2 | 648.00 | 1.5032 | 5.35160 | 2024.30 | 30.090 |
| 3 | 648.00 | 1 | 6.68870 | 2024.30 | 30.553 |
| 4 | 518.40 | 0.5974 | 6.68870 | 1620.40 | 29.858 |
| PU 4 | | | | | |
| 1 | 466.56 | 1 | 4.81670 | 1458.90 | 28.847 |
| 2 | 583.20 | 1.5033 | 4.81670 | 1822.40 | 29.543 |
| 3 | 583.20 | 1 | 6.02010 | 1822.30 | 30.006 |
| 4 | 466.56 | 0.5974 | 6.02010 | 1458.90 | 29.311 |
| PU 5 | | | | | |
| 1 | 419.90 | 1 | 4.33530 | 1313.50 | 28.300 |
| 2 | 524.88 | 1.5033 | 4.33530 | 1640.60 | 28.996 |
| 3 | 524.88 | 1 | 5.41840 | 1640.60 | 29.459 |
| 4 | 419.90 | 0.5974 | 5.41840 | 1313.50 | 28.764 |
| PU 6 | | | | | |
| 1 | 377.91 | 1 | 3.90210 | 1182.70 | 27.753 |
| 2 | 472.39 | 1.5033 | 3.90210 | 1477.10 | 28.448 |
| 3 | 472.39 | 1 | 4.87690 | 1477.10 | 28.912 |
| 4 | 377.91 | 0.5974 | 4.87690 | 1182.70 | 28.216 |
| PU 7 | | | | | |
| 1 | 340.12 | 1 | 3.51230 | 1064.90 | 27.206 |
| 2 | 425.15 | 1.5033 | 3.51230 | 1329.90 | 27.901 |
| 3 | 425.15 | 1 | 4.38950 | 1329.90 | 28.365 |
| 4 | 340.12 | 0.5974 | 4.38950 | 1064.90 | 27.669 |

Table 6 depicts the results of the case studies carried out with data from Table 5 with real helium used as the working fluid. The seven PUs coupled in cascade are included. Each PU is composed of two RDACs, each equipped with internal regenerative piping equipment not available in symbolic mode.

Table 6: Results of case studies with the data from Table 5 for the irreversible internally regenerative VTVT cycle in terms of performance focused on the SFI as a function of the RIT, assuming an internal heat regeneration factor of RF =0.5 = 50% and an LF of 0.9, with helium as the working fluid

| I/O | row | Test –for He | PU1 | PU2 | PU3 | PU4 | PU5 | PU6 | PU7 |
|---|---|---|---|---|---|---|---|---|---|
| Input data | 1 | TH [K] | 800.00 | 720.00 | 648.00 | 583.20 | 524.88 | 472.39 | 425.15 |
| | 2 | TL [K] | 640.00 | 576.00 | 518.40 | 466.56 | 419.90 | 377.91 | 340.12 |
| | 3 | RIT[[$T_1/T_2$] | 0.80 | 0.80 | 0.80 | 0.80 | 0.80 | 0.80 | 0.80 |
| | 4 | LF | 0.90 | 0.90 | 0.90 | 0.90 | 0.90 | 0.90 | 0.90 |
| | 5 | RF | 0.50 | 0.50 | 0.50 | 0.50 | 0.50 | 0.50 | 0.50 |

| | | | | | | | | | |
|---|---|---|---|---|---|---|---|---|---|
| ta | 6 | $p_{ref}$ [bar] | 1 | 1 | 1 | 1 | 1 | 1 | 1 |
| Output data | 7 | $q_{i_}$12+23[kJ] $kg^{-1}$ | 832.68 | 748.72 | 673.92 | 606.52 | 545.82 | 491.67 | 442.54 |
| | 8 | $q_{i\_ext}$ [kJ] $kg^{-1}$ | 583.38 | 524.37 | 471.97 | 424.82 | 382.27 | 344.47 | 310.04 |
| | 9 | $q_{o_}$34+41 [kJ] $kg^{-1}$ | 765.29 | 688.72 | 620.38 | 558.24 | 502.45 | 451.88 | 406.73 |
| | 10 | $q_{\_reg}$ [kJ] $kg^{-1}$ | 249.30 | 224.35 | 201.95 | 181.70 | 163.55 | 147.20 | 114.42 |
| | 11 | $w_o$23 [kJ] $kg^{-1}$ | 334.08 | 300.02 | 270.02 | 243.02 | 218.72 | 197.27 | 177.54 |
| | 12 | $w_o$41 [kJ] $kg^{-1}$ | 266.69 | 240.02 | 216.48 | 194.84 | 175.35 | 157.48 | 141.73 |
| | 13 | $\eta_{th\_exp}$ [%] | 40.12 | 40.07 | 40.07 | 40.07 | 40.07 | 40.07 | 40.07 |
| | 14 | $\eta_{th\_contr}$ [%] | 34.85 | 34.85 | 34.90 | 34.90 | 34.90 | 34.90 | 34.90 |
| | 15 | $w_n$ [kJ] $kg^{-1}$ | 667.52 | 600.05 | 540.56 | 486.51 | 437.85 | 394.16 | 354.75 |
| | 16 | $\eta_{th\_reg}$ [%] | 114.42 | 114.43 | 114.53 | 114.52 | 114.54 | 114.43 | 114.42 |
| | 17 | $\eta_{th}$ [%]) | 80.17 | 80.14 | 80.21 | 80.21 | 80.22 | 80.17 | 80.16 |
| | 18 | SFI [%] | 14.42 | 14.43 | 14.53 | 14.52 | 14.54 | 14.43 | 14.42 |

The results of the PUs shown in Table 6 include the input and output parameters that can be compared between each case such that they indicate trends that are interesting for the implementation of prototypes. Thus, such trends will be taken into account in the results analysis section to establish useful design criteria.

Table 7 depicts the data resulting from the irreversible VTVT cycle analysis for a PP consisting of seven PUs with internal heat regeneration connected in the cascade depicted in Figure 7(b). The values of the inlet/outlet temperatures of each PU coupled in cascade are similar to those used in the plant that operates with helium according to Figure 7(a). Nevertheless, the values that result from processing the VTVT cycle with air as TWF produce values of other very different parameters. Therefore, the results of the analysis of air as a TWF are different and unique to air.

As in the case of helium as a working fluid, a greater amount of useful low-grade heat remains in the thermal cooling fluid because more than half of the heat rejected by the VTVT cycle cannot be recovered in an amount greater than that for helium since irreversibilities are greater for air than for helium. Then, it could be used through a feeding system for another cascade of PUs, which would significantly increase the regenerative efficiency of the power plant. As in the case of helium, this case study is not considered in this work.

Table 7: Data resulting from the VTVT cycle analysis for a PP consisting of a cascade of seven PUs with internal heat regeneration focused on the SFI as a function of the RIT assuming an internal heat regeneration factor of 0.5 = 50%, a losses factor of 0.9, and real air as the working fluid

| PU 1 | | | | | |
|---|---|---|---|---|---|
| SPs | *T*[K] | p[bar] | *v*[kJ.$kg^{-1}$] | *u*[kJ.$kg^{-1}$] | *s*[kJ.$kg^{-1}$.K] |
| 1 | 640.00 | 1 | 0.91340 | 591.94 | 4.4665 |
| 2 | 800.00 | 1.5037 | 0.91340 | 718.79 | 4.6433 |
| 3 | 800.00 | 1 | 1.14170 | 718.79 | 4.7074 |
| 4 | 640.00 | 0.5972 | 1.14170 | 591.94 | 4.5307 |
| PU 2 | | | | | |
| 1 | 576.00 | 1 | 0.82205 | 542.90 | 4.3555 |
| 2 | 720.00 | 1.5039 | 0.82205 | 654.58 | 4.5284 |
| 3 | 720.00 | 1 | 1.02760 | 654.58 | 4.5926 |
| 4 | 576.00 | 0.5970 | 1.02760 | 542.90 | 4.4197 |
| PU 3 | | | | | |
| 1 | 518.40 | 1 | 0.73981 | 499.54 | 4.2459 |

| | | | | | |
|---|---|---|---|---|---|
| 2 | 648.00 | 1.5039 | 0.73981 | 598.10 | 4.4155 |
| 3 | 648.00 | 1 | 0.92481 | 598.10 | 4.4797 |
| 4 | 518.40 | 0.5971 | 0.92481 | 499.54 | 4.3101 |
| PU 4 | | | | | |
| 1 | 466.56 | 1 | 0.66577 | 461.09 | 4.1375 |
| 2 | 583.20 | 1.5041 | 0.66577 | 548.33 | 4.3043 |
| 3 | 583.20 | 1 | 0.83232 | 548.33 | 4.3685 |
| 4 | 466.56 | 0.5970 | 0.83232 | 461.09 | 4.2017 |
| PU 5 | | | | | |
| 1 | 419.90 | 1 | 0.59911 | 426.87 | 4.0299 |
| 2 | 524.88 | 1.5043 | 0.59911 | 504.34 | 4.1945 |
| 3 | 524.88 | 1 | 0.74906 | 504.34 | 4.2588 |
| 4 | 419.90 | 0.5964 | 0.74906 | 426.87 | 4.0942 |
| PU 6 | | | | | |
| 1 | 377.91 | 1 | 0.53908 | 396.33 | 3.9230 |
| 2 | 472.39 | 1.5046 | 0.53908 | 465.34 | 4.0859 |
| 3 | 472.39 | 1 | 0.67410 | 465.39 | 4.1502 |
| 4 | 377.91 | 0.5967 | 0.67410 | 396.39 | 3.9873 |
| PU 7 | | | | | |
| 1 | 340.12 | 1 | 0.48502 | 369.00 | 3.8164 |
| 2 | 425.15 | 1.5050 | 0.48502 | 430.64 | 3.9782 |
| 3 | 425.15 | 1 | 0.60661 | 430.64 | 4.0426 |
| 4 | 340.12 | 0.5965 | 0.60661 | 369.00 | 3.8809 |

Table 8 depicts the results of the case studies carried out with data from Table 7 for real air as the working fluid. The seven PUs coupled in cascade are included. As in the cases when helium is used as the working fluid, each PU is composed of two RDACs, each equipped with internal regenerative piping equipment not available in symbolic mode.

Table 8: Results of the case studies with data from Table 7 for the irreversible internally regenerative VTVT cycle in terms of performance focused on the SFI as a function of the RIT, assuming an internal heat regeneration factor of RF = 0.5 = 50%, a losses factor of 0.9, and air as the working fluid

| I/O | row | Test -Air | PU1 | PU2 | PU3 | PU4 | PU5 | PU6 | PU7 |
|---|---|---|---|---|---|---|---|---|---|
| Input data | 1 | TH [K] | 800.00 | 720.00 | 648.00 | 583.20 | 524.88 | 472.39 | 425.15 |
| | 2 | TL [K] | 640.00 | 576.00 | 518.40 | 466.56 | 419.90 | 377.91 | 340.12 |
| | 3 | RIT[$[T_1/T_2]$ | 0.80 | 0.80 | 0.80 | 0.80 | 0.80 | 0.80 | 0.80 |
| | 4 | LF | 0.9 | 0.9 | 0.9 | 0.9 | 0.90 | 0.90 | 0.90 |
| | 5 | RF | 0.5 | 0.5 | 0.5 | 0.5 | 0.50 | 0.50 | 0.50 |
| | 6 | $p_{ref}$ [bar] | 1 | 1 | 1 | 1 | 1 | 1 | 1 |
| Output | 7 | $q_{i_}$12+23[kJ] $kg^{-1}$ | 173.00 | 153.28 | 136.00 | 120.94 | 0.75 | 0.67 | 0.61 |
| | 8 | $q_{i\_ext}$ [kJ] $kg^{-1}$ | 109.58 | 97.44 | 86.72 | 77.32 | 69.11 | 61.85 | 55.46 |
| | 9 | $q_{o_}$34+41 [kJ] $kg^{-1}$ | 163.83 | 144.96 | 128.51 | 114.20 | 101.77 | 90.87 | 81.38 |
| | 19 | $q_{\_reg}$ [kJ] $kg^{-1}$ | 63.43 | 55.84 | 49.28 | 43.62 | 38.74 | 34.50 | 30.82 |

| | | | | | | | | | |
|---|---|---|---|---|---|---|---|---|---|
| d a t a | 11 | $w_o23$ [kJ] $kg^{-1}$ | 46.15 | 41.60 | 37.44 | 33.70 | 30.37 | 27.34 | 24.64 |
| | 12 | $w_o41$ [kJ] $kg^{-1}$ | 36.98 | 33.28 | 29.95 | 26.96 | 24.30 | 21.87 | 19.74 |
| | 13 | $\eta_{th\_exp}$ [%] | 173.00 | 153.28 | 136.00 | 120.94 | 0.75 | 0.67 | 0.61 |
| | 14 | $\eta_{th\_contr}$ [%] | 109.58 | 97.44 | 86.72 | 77.32 | 69.11 | 61.85 | 55.46 |
| | 15 | $w_n$ [kJ] $kg^{-1}$ | 53.39 | 54.28 | 55.06 | 55.73 | 56.33 | 56.75 | 57.16 |
| | 16 | $\eta_{th\_reg}$ [%] | 84.30 | 85.39 | 86.35 | 87.17 | 87.90 | 88.40 | 88.92 |
| | 17 | $\eta_{th}$ [%]) | 53.39 | 54.28 | 55.06 | 55.73 | 56.33 | 56.75 | 57.16 |
| | 18 | SFI [%] | -15.70 | -14.61 | -13.65 | -12.83 | -12.10 | -11.60 | -11.08 |

The results of the PUs shown in Table 8 include the input and output parameters that can be compared between each case studied such that they indicate trends that are interesting for the implementation of prototypes. Thus, in the results analysis section, such trends will be taken into account to establish useful design criteria. Furthermore, the comparison of the results of Table 6 for helium and Table 8 for air will provide useful information about different working fluids.

### 3.3 Self-powered power plant based on irreversible externally regenerative PUs coupled in a series of cascaded PUs using helium as the working fluid

The PP designed to operate with external heat regeneration consists of a series of three cascaded groups of PUs depicted in Figure 8. The first cascaded group of PUs is represented in Table 9. The second cascaded group of PUs is represented in Table 10, and the third cascaded group of PUs is represented in Table 11.

According to the PP scheme depicted in Figure 8, the rejected heat (low-grade heat that cannot be used in the previous cycle) by the first group of cascaded PUs is contained in the thermal cooling fluid. This fluid is used as the heat transporter to supply heat to the second group of cascaded PUs. Meanwhile, the heat rejected by the second group of cascaded PUs to the thermal cooling fluid is used as the heat transporter to supply heat to the third and last PU. As a consequence, the rejected heat from the last PU consists of very low-grade heat and, therefore, is useless and negligible.

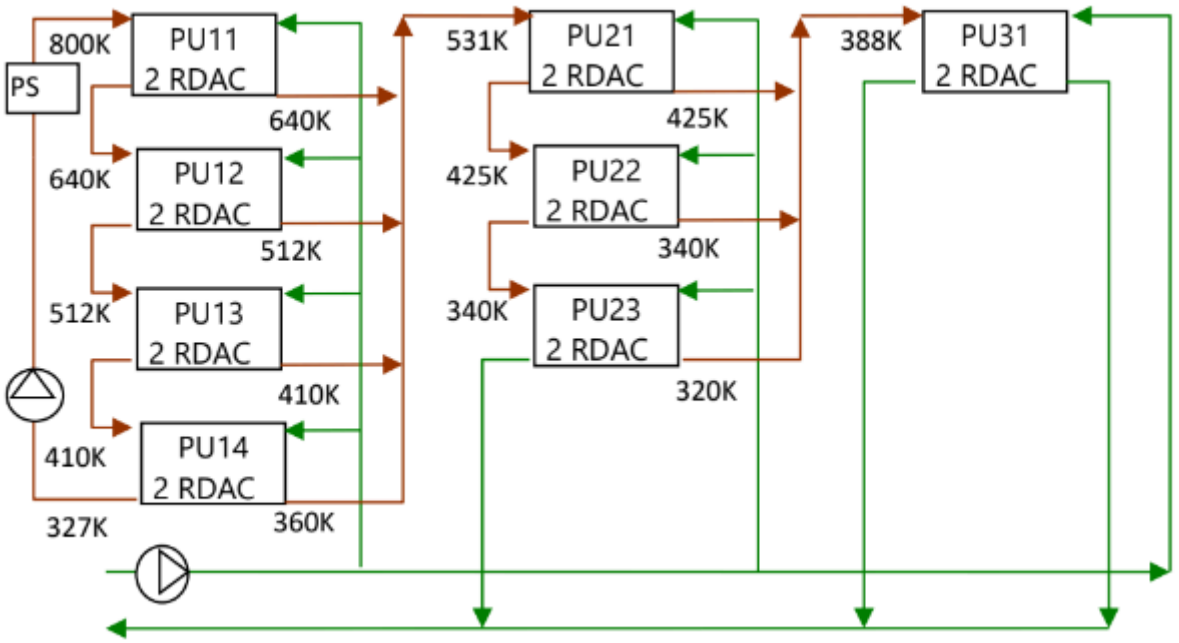


Figure 8: Case study consisting of externally regenerative PP structure based on a series of three cascaded groups of PUs operated by irreversible VTVT cycles with helium as the working fluid. External heat regeneration is based on using the heat recovered from the first cascaded group and is used in the next downstream PUs.

Table 9: Data resulting from the irreversible VTVT cycle analysis for the first cascaded group of four PUs equipped with a heat recovery system destined to feed the next group of three PUs focusing on the SFI as a function of the RIT assuming an external heat regeneration factor of RF = 0.9 = 90% of the available heat and an LF of 0.9, with real helium as the working fluid

| PU 11 | | | | | |
|---|---|---|---|---|---|
| SPs | *T*[K] | p[bar] | *v*[kJ.kg$^{-1}$] | *u*[kJ.kg$^{-1}$] | *s*[kJ.kg$^{-1}$.K] |
| 1 | 640.00 | 1 | 6.60610 | 1999.30 | 30.489 |
| 2 | 800.00 | 1.5033 | 6.60610 | 2497.90 | 31.184 |
| 3 | 800.00 | 1 | 8.25690 | 2497.90 | 31.648 |
| 4 | 640.00 | 0.5974 | 8.25690 | 1999.30 | 30.952 |
| PU 12 | | | | | |
| 1 | 512.00 | 1 | 5.28550 | 1600.50 | 29.330 |
| 2 | 640.00 | 1.5033 | 5.28550 | 1999.30 | 30.025 |
| 3 | 640.00 | 1 | 6.60610 | 1999.30 | 30.489 |
| 4 | 512.00 | 0.5974 | 6.60610 | 1600.50 | 29.793 |
| PU 13 | | | | | |
| 1 | 409.60 | 1 | 4.22910 | 1281.40 | 28.171 |
| 2 | 512.00 | 1.5032 | 4.22910 | 1600.50 | 28.867 |
| 3 | 512.00 | 1 | 5.28550 | 1600.50 | 29.330 |
| 4 | 409.60 | 0.5974 | 5.28550 | 1281.40 | 28.635 |
| PU 14 | | | | | |
| 1 | 327.68 | 1 | 3.38390 | 1026.10 | 27.012 |
| 2 | 409.60 | 1.5033 | 3.38390 | 1281.40 | 27.708 |
| 3 | 409.60 | 1 | 4.22910 | 1281.40 | 28.171 |
| 4 | 327.68 | 0.5974 | 4.22910 | 1026.10 | 27.476 |

Table 10: Data resulting from the irreversible VTVT cycle analysis for the second cascaded group of three PUs fed with the heat recovered from the previous group of PUs equipped with a heat recovery system destined to feed the next group of one PU focused on the SFI as a function of the RIT, assuming an external heat regeneration factor of RF = 0.8 = 80% of the available heat and an LF of 0.9, with real helium as the working fluid

| PU 21 | | | | | |
|---|---|---|---|---|---|
| SPs | *T*[K] | p[bar] | *v*[kJ.kg$^{-1}$] | *u*[kJ.kg$^{-1}$] | *s*[kJ.kg$^{-1}$.K] |
| 1 | 425.09 | 1 | 4.38890 | 1329.70 | 28.364 |
| 2 | 531.36 | 1.5032 | 4.38890 | 1660.80 | 29.059 |
| 3 | 531.36 | 1 | 5.48530 | 1660.80 | 29.523 |
| 4 | 425.09 | 0.5974 | 5.48530 | 1329.70 | 28.827 |
| PU 22 | | | | | |
| 1 | 340.07 | 1 | 3.51170 | 1064.70 | 27.205 |
| 2 | 425.09 | 1.5033 | 3.51170 | 1329.70 | 27.900 |
| 3 | 425.09 | 1 | 4.38890 | 1329.70 | 28.364 |
| 4 | 340.07 | 0.5974 | 4.38890 | 1064.70 | 27.669 |
| PU 23 | | | | | |
| 1 | 272.06 | 1 | 2.81010 | 852.81 | 26.046 |
| 2 | 340.07 | 1.5032 | 2.81010 | 1064.80 | 26.742 |
| 3 | 340.07 | 1 | 3.51170 | 1064.80 | 27.205 |

| | | | | | |
|---|---|---|---|---|---|
| 4 | 272.06 | 0.5974 | 3.51170 | 852.81 | 26.510 |

Table 11: Data resulting from the irreversible VTVT cycle analysis for the third cascaded group of one PU fed with the heat recovered from the previous group focused on the SFI as a function of the RIT, assuming an external heat regeneration factor of RF = 0.7 = 70% of the available heat and an LF of 0.9, with real helium as the working fluid

| PU 31 | | | | | |
|---|---|---|---|---|---|
| SPs | *T*[K] | p[bar] | *v*[kJ.kg$^{-1}$] | *u*[kJ.kg$^{-1}$] | *s*[kJ.kg$^{-1}$.K] |
| 1 | 311.16 | 1 | 3.21350 | 974.65 | 26.744 |
| 2 | 388.96 | 1.5033 | 3.21350 | 1217.10 | 27.439 |
| 3 | 388.96 | 1 | 4.01610 | 1217.10 | 27.903 |
| 4 | 311.16 | 0.5974 | 4.01610 | 974.65 | 27.207 |

Table 12 shows the results of the analysis for the PP structured as a series of three cascaded groups of PUs depicted in Tables 9, 10, and 11 with values of RF = 0.9, 0.8, and 0.7 and real helium as the working fluid.

Table 12: Results of the analysis for the PP structured as a three series of cascaded groups of PUs from the analysis of the data in Tables 9, 10, and 11 for RF values of 0.9, 0.8, and 0.7 with real helium as the working fluid

| | I/O parameters | table 9 | Table 10 | Table 11 |
|---|---|---|---|---|
| input data | RIT= | 0.9 | 0.9 | 0.9 |
| | LF= | 0.9 | 0.9 | 0.9 |
| | RF= | 0.9 | 0.8 | 0.7 |
| output data | $\eta_{\_reg}$= | 124.34 | 114 | 108 |
| | SFI [%] = | 24.34 | 14 | 8 |

Table 12 shows the results of the PP for several RF values. As a consequence, three values of the SFI were achieved: 24.34, 14.0, and 8.0. In the worst case considered, an SFI of 8 MW is achieved. This means that a PP designed to supply 100 MW of nominal power can operate without external heat, supplying 8 MW at free cost.

The analysis of the results indicated in the next section shows that no great or relevant differences exist with respect to the studied cases concerning internal heat regeneration in terms of the SFI.

**4 Analysis of results**

The formal foundations of the study described in this article originate in the equality of Equation (9), which is responsible describing essential properties of the VTVT cycle, through which essential theorems are deduced. Consequently, the deduction of Equation (9) constitutes the basis for achieving the empirical demonstration of both theorems, according to Equations (12a)–(12f), given that it is supported by irrefutable empirical evidence.

The results are related to the proposed case studies intended for designing viable self-powered prototypes. The analysis of the proposed case studies adheres to the flowing theorems and associated corollaries: the theorem of the maximum value of the RIT, the theorem of functional efficiency dependence of the RIT, and the theorem of the maximum value of the SFI.

The consequences of both theorems allow us to find a set of plant parameters and the operation conditions under which a compromise can be achieved between specific work, thermal efficiency, and SFI.

Table 4 depicts the data from the ideal VTVT cycle analysis using the data depicted in Table 3. As the RIT increases, the thermal efficiency, regenerative thermal efficiency, and the SFI also increase while net work consequently decreases significantly. The objective was to achieve the performance as a function of the RIT for a group of six ideal cases characterized by the absence of irreversibilities subjected to the highest and unachievable SFI.

Table 13: Results of the analysis of six cases of the reversible regenerative VTVT cycle operating with RIT values from 0.99 to 0.5.

| Test | 1 | 2 | 3 | 4 | 5 | 6 |
|---|---|---|---|---|---|---|
| TH [K] | 800.00 | 800.00 | 800.00 | 800.00 | 800.00 | 800.00 |

| | | | | | | |
|---|---|---|---|---|---|---|
| TL [K] | 792.00 | 784.00 | 760.00 | 720.00 | 560.00 | 400.00 |
| RIT*100 | 99.00 | 98.00 | 95.00 | 90.00 | 70.00 | 50.00 |
| $w_n$ [kJ.kg$^{-1}$] | 33.43 | 66.53 | 166.92 | 332.88 | 1007.76 | 1728.00 |
| $\eta_{\_reg}$ [%] | 199.00 | 198.00 | 195.00 | 190.00 | 170.00 | 164.24 |
| $\eta_{th}$ [%] | 79.98 | 79.67 | 79.37 | 78.42 | 75.17 | 72.05 |
| SFI | 99.00 | 98.00 | 95.00 | 90.00 | 70.00 | 64.24 |

The examination of the behavior of the disruptive ideal reversible regenerative VTVT cycle at different RIT values provides outstanding conclusions concerning design criteria in terms of efficiency as shown in Table 4 and summarized in Table 13. The results in Table 13 agree with the limitations imposed by Theorem 2. However, the maximum RIT value for the VTVT cycle cannot approach unity, meaning it must be less than 1 to be effective. This constraint follows the corollary of Theorem 2. The greater the RIT, the closer it is to unity. Moreover, the greater the ratio of useful works, the greater the thermal efficiency of the VTVT cycle.

Ideally, as the RIT approaches 1, the thermal efficiency of the ideal regenerative VTVT cycle approaches 200%. Consequently, the SFI approaches 100%. However, under practical (real) conditions, SFI cannot reach 100% due to the inherent irreversibilities and the restriction imposed to the RIT, which must satisfy the inequality RIT < 1 or RIT < 100%.

**4.1 Results for an irreversible internally regenerative VTVT cycle**

This case study consists of a power plant comprising seven irreversible PUs operating with internal regeneration such that the RF is assumed to be 0.5, the LF is 0.9, and the RIT is 0.9.

Table 14: Relevant results of the analysis depicted in Table 6 for helium as the working fluid and Table 8 for air as the working fluid.

| Helium as working fluid | | | | | | | |
|---|---|---|---|---|---|---|---|
| Parameter | PU1 | PU2 | PU3 | PU4 | PU5 | PU6 | PU7 |
| TH [K] | 800.00 | 720.00 | 648.00 | 583.20 | 524.88 | 472.39 | 425.15 |
| TL [K] | 640.00 | 576.00 | 518.40 | 466.56 | 419.90 | 377.91 | 340.12 |
| RIT[$[T_1/T_2]$ | 0.80 | 0.80 | 0.80 | 0.80 | 0.80 | 0.80 | 0.80 |
| LF | 0.90 | 0.90 | 0.90 | 0.90 | 0.90 | 0.90 | 0.90 |
| RF | 0.50 | 0.50 | 0.50 | 0.50 | 0.50 | 0.50 | 0.50 |
| $w_n$ [kJ] kg$^{-1}$ | 667.52 | 600.05 | 540.56 | 486.51 | 437.85 | 394.16 | 354.75 |
| $\eta_{th\_reg}$ [%] | 114.42 | 114.43 | 114.53 | 114.52 | 114.54 | 114.43 | 114.42 |
| $\eta_{th}$ [%]) | 80.17 | 80.14 | 80.21 | 80.21 | 80.22 | 80.17 | 80.16 |
| SFI [%] | 14.42 | 14.43 | 14.53 | 14.52 | 14.54 | 14.43 | 14.42 |
| Air as working fluid | | | | | | | |
| Parameter | PU1 | PU2 | PU3 | PU4 | PU5 | PU6 | PU7 |
| TH [K] | 800.00 | 720.00 | 648.00 | 583.20 | 524.88 | 472.39 | 425.15 |
| TL [K] | 640.00 | 576.00 | 518.40 | 466.56 | 419.90 | 377.91 | 340.12 |
| RIT[$[T_1/T_2]$ | 0.80 | 0.80 | 0.80 | 0.80 | 0.80 | 0.80 | 0.80 |
| LF | 0.9 | 0.9 | 0.9 | 0.9 | 0.90 | 0.90 | 0.90 |
| RF | 0.5 | 0.5 | 0.5 | 0.5 | 0.50 | 0.50 | 0.50 |
| $w_n$ [kJ] kg$^{-1}$ | 53.39 | 54.28 | 55.06 | 55.73 | 56.33 | 56.75 | 57.16 |
| $\eta_{th\_reg}$ [%] | 84.30 | 85.39 | 86.35 | 87.17 | 87.90 | 88.40 | 88.92 |
| $\eta_{th}$ [%]) | 53.39 | 54.28 | 55.06 | 55.73 | 56.33 | 56.75 | 57.16 |
| SFI [%] | -15.70 | -14.61 | -13.65 | -12.83 | -12.10 | -11.60 | -11.08 |

Table 14 shows that an average SFI value of 14.4 was obtained with helium as the real working fluid, while a negative SFI (varying from -15.7 to -11.8) was obtained with air as the real working fluid as a function of the top temperatures. This is the essential difference between the results when helium or air is used as the working fluid. This result shows that using air as a working fluid is not advisable in the case of internal regeneration. However, satisfactory results were obtained for helium since a power plant designed to supply 100 MW can provide an SFI of 14.4%, which is equivalent to 14.4 MW when operating without adding external heat.

As the reader has probably observed, the previous results could be improved by simply changing the RIT value from 0.8 to 0.85 or 0.9. We studied a case with an RIT of 0.8 because the mechanical structure of the prototype requires a smaller number of PUs. That is, the number of PUs grows with the RIT since the higher the value of the RIT, the smaller the temperature gradients ($T_2$-$T_1$) of each PU and, consequently, the greater the number of PUs necessary to achieve the design power.

The SFI value was in the case of internal regeneration due to the impossibility of regenerating more than 50% of the available heat in the ideal case. Nevertheless, an important fraction of the heat rejected could be recovered by the heat recovery system that transports the cooling fluid to a heat sink. This is feasible because this VTVT thermal cycle is characterized by operating at high performance with low-temperature gradients (high RIT) and at a low temperature $T_2$ at the same time. Therefore, the addition of PUs is possible without external heat input, which enhances the efficiency of PP.

**4.2 Results for an irreversible externally regenerative VTVT cycle**

The results of the analysis for the PP structured as a series of three cascaded groups of PUs depicted in Figure 8 from the analysis of data Tables 9, 10, and 11 for values of the RF of 0.9, 0.8, and 0.7 with helium as the working fluid yields results coherent with the previous analysis carried out previously. A summary of Table 12 indicates that a PP equipped with external heat regeneration and structured according to the scheme depicted in Figure 8 delivers efficiencies of 124.34%, 114%, and 108% as a function of the RF of 0.9, 0.8, and 07, respectively. This means that such a PP could be used as a self-powered engine delivering SFI values of 24.34%, 14%, and 8%, respectively.

The results of the previous analysis highlight that the heat recovery factor plays a relevant role since, with a recovery factor of 0.9, net work is obtained without the external addition of heat of the order of 24% of the nominal design power. Meanwhile, with a heat recovery factor of 0.7, only 8% of the nominal design power would be obtained. The results show also that this extraordinary efficiency confirms the technical viability of real machines that exhibit the ability to provide more energy than they use, that is, second-class perpetual motion machines.

**5 Conclusions**

The proposed disruptive cycle enabled the implementation of a disruptive self-powered PP that can integrate strictly isothermal closed processes within thermal VTVT-based thermal cycles, which can convert heat and cold into useful mechanical work via two facilities: closed isothermal expansion. It does this by adding heat and closed isothermal contraction or vacuum by extracting heat at no cost. However, this technique alone cannot achieve the objectives imposed by a self-powered PP because it is not possible to achieve such high efficiency without completely recovering the rejected heat.

Furthermore, using conventional thermodynamics based on the restrictions imposed by Carnot's theorem would not be viable. Vacuum techniques (double-effect thermal contraction by cooling at zero cost) have been used to overcome this drawback. The strategy used to solve a problem that until now was unsolvable due to the restrictions imposed by conventional thermodynamics represents a technical and theoretical disruptive solution consisting of a study design aiming to prototype self-powered PPs. A rigorous and consistent analysis of the proposed thermal cycle has been performed. Applied theory follows empirical and observational evidence, and the consistency of the analysis is supported by the corresponding theorems and their associated corollaries: the theorem of the maximum value of the RIT, the theorem of the efficiency dependence of the RIT, and the theorem of the maximum value of the SFI.

Some case studies have been developed and analyzed as a consequence of modeling two regenerative strategies (internal and external). The findings derived from the case studies enable the development and implementation of several prototypes under a wide range of presumably viable alternatives. The most relevant findings deal with the possibility of prototyping self-powered PPs so that the contribution of heat from an external source is unnecessary. This means that energy can be obtained autonomously by simply having the thermal power plant and a fee-cost residual heat sink.

In accordance with the results in Tables 13 and 14, there is a great difference in efficiency between the results achieved in regenerative plants equipped with ideal cycles and the results obtained in plants equipped with irreversible thermal cycles. Such unwanted differences in efficiency highlight the need to make the maximum effort possible to reduce mechanical and thermal losses in all aspects related to heat transfer through prototyping-based evidence. In summary, this article constitutes an incentive to encourage potential entrepreneurs to build prototypes prior to authorization based on the findings subject to patent rights.

Finally, it is worth mentioning that with the strategy used in heat management, perpetual motion machines of the second class are achieved. These results lead to the need to review some fundamental principles of classical thermodynamics that affect conventional physics.

Likewise, researchers, venture capital investors, startups and entrepreneurs are given the opportunity to request technical-scientific assistance as well as license agreements for patent P202200035 with publication number ES2956342A2 to create and exploit at least one of six patented prototypes.

**References**

[1] Wikipedia. Thomas Savery. https://en.wikipedia.org/wiki/Thomas_Savery.

[2] Wikipedia. Thomas Newcomen. https://en.wikipedia.org/wiki/Thomas_Newcomen;

[3] Wikipedia. James Watt: https://en.wikipedia.org/wiki/James_Watt; and https://en.wikipedia.org/wiki/Watt_steam_engine.

[4] J.G. van der Kooij. "The Invention of the Steam Engine" Version 1.1 (January 2015) SBN-10: 1502809095 ISBN-13: 978-1502809094. Copyright © 2015 B. J. G. van der Kooij. Available on: The_Invention_of_the_Steam_Engine_TU-Delft_Edition (2).pdf; Available on: http://resolver.tudelft.nl/uuid:8ac197ad-d898-4698-bedc-53983af87b84; Available on: https://repository.tudelft.nl/islandora/object/uuid:8ac197ad-d898-4698-bedc-53983af87b84/datastream/OBJ/download;

[5] Nuvolari. Alessandro. "The making of steam power technology". A Study of Technical Change during the British Industrial Revolution. Eindhoven: Technische Universiteit Eindhoven. 2004. –Proefschrift- . ISBN 90-386-2077-2. Printing: Eindhoven University Press. Available on: https://www.iris.sssup.it/bitstream/11382/303321/1/MakingFinal.pdf;

[6] Müller. Gerald. The atmospheric steam engine as energy converter for low and medium temperature thermal energy. Renewable energy. 2013. vol. 53. p. 94-100. https://doi.org/10.1016/j.renene.2012.10.056;

[7] Gerald Müller. George Parker. Experimental investigation of the atmospheric steam engine with forced expansion. Renewable Energy. Vol. 75. 2015. pp 348-355. ISSN 0960-1481. https://doi.org/10.1016/j.renene.2014.09.061; https://www.sciencedirect.com/science/article/pii/S0960148114006375.

[8] Vítor Augusto Andreghetto Bortolin. Bernardo Luiz Harry Diniz Lemos. Rodrigo de Lima Amaral. Cesar Monzu Freire & Julio Romano Meneghini. Thermodynamical model of an atmospheric steam engine. Journal of the Brazilian Society of Mechanical Sciences and Engineering Vol. 43. 493 (2021). https://doi.org/10.1007/s40430-021-03209-9

[9] Knowlen C. Williams J. Mattick A. Deparis H. Hertzberg A. Quasi-isothermal expansion engines for liquid nitrogen automotive propulsion. 1997. SAE paper 972649. https://www.doi.org/10.4271/972649.

[10] Cicconardi S. Jannelli E. Perna A. Spazzafumo G. A steam cycle with an isothermal expansion: the effect of flow variation. Int J Hydrogen Energy 1999;24(1):53-57 https://www.doi.org/10.1016/S0360-3199(98)00011-1.

[11] Cicconardi S. Jannelli E. Perna A. Spazzafumo G. Parametric analysis of a steam cycle with a quasi-isothermal expansion. Int J Hydrogen Energy 2001;26(3): 275-279. https://www.doi.org/10.1016/S0360-3199(00)00036-7.

[12] Park JK. Ro PI. Lim SD. Mazzoleni AP. Quinlan B. Analysis and optimization of a quasi-isothermal compression and expansion cycle for ocean compressed air energy storage (OCAES). In: Oceans. 2012. IEEE; 2012. pp. 1-8

https://www.doi.org/10.1109/OCEANS.2012.6404964.

[13] Kim Y-M. Shin D-G. Lee S-Y. Favrat D. Isothermal transcritical CO2 cycles with TES (thermal energy storage) for electricity storage. Energy 2013;49: 484-501. https://www.doi.org/10.1016/j.energy.2012.09.057

[14] Opubo N. Igobo. Philip A. Davies. A high-efficiency solar Rankine engine with isothermal expansion. Int J Low-Carbon Technol. 2013; 8(Suppl. 1):i27-33. https://www.doi.org/10.1093/ijlct/ctt031.

[15] Opubo N. Igobo. Philip A. Davies. Review of low-temperature vapor power cycle engines with quasi-isothermal expansion. Energy 70 (2014) 22-34. https://www.doi.org/10.1016/j.energy.2014.03.123

[16] Ferreiro R. Ferreiro B. Isothermal and Adiabatic Expansion Based Trilateral Cycles. British Journal of Applied Science & Technology. 2015; (8) 5: 448-460. https://www.doi.org/10.9734/BJAST/2015/17350

[17] Ferreiro R.. Ferreiro B.. The Behavior of Some Working Fluids Applied on the Trilateral Cycles with Isothermal Controlled Expansion. British Journal of Applied Science & Technology. 2015; (9) 5: 694 450-463.

https://www.doi.org/10.9734/BJAST/2015/18624

[18] Ramon Ferreiro Garcia. Jose Carbia Carril, Closed Processes Based Heat-Work Interactions Doing Useful Work by Adding and Releasing Heat. International Journal of Emerging Engineering Research and Technology.

Volume 6. Issue 11. 2018. pp 8-23. ISSN 2349-4395 (Print) & ISSN 2349-4409 (Online). Accessed at: https://www.ijeert.org/papers/v6-i11/2.pdf; https://www.ijeert.org/v6-i11.

[19] R. Ferreiro Garcia, Power Pants and Cycles: Advances and Trends, Book Publisher International, London 2020, ISBN-13 (15) 978-93-90431-67- 0; https://doi.org/10.9734/bpi/mono/978-93-90431-59-5; http://bp.bookpi.org/index.php/bpi/catalog/book/332; https://www.doi.org/10.9734/bpi/mono/978-93-90431-59-5.

[20] Meeta Sharma. Onkar Singh. Parametric Evaluation of HRSG. Heat Transfer. Volume 43. Issue 8. 2014. Pages 691-705. https://doi.org/10.1002/htj.21106.

[21] Meeta Sharma. Onkar Singh. Exergy Based Parametric Analysis of a Heat Recovery Steam Generator. Heat Transfer. Volume 45. Issue 1. 2016. Pages1-14. https://doi.org/10.1002/htj.21148.

[22] Ramon Ferreiro Garcia, Jose Carbia Carril. Combined Cycle Consisting of Closed Processes Based Cycle Powered by A Reversible Heat Pump that Exceed Carnot Factor. Journal of Advances in Physics, Volume 15, (2018), Pages: 6078-6100. ISSN: 2347-3487. DOI: 10.24297/jap.v15i0.8034; Accessed at: Combined Cycle Consisting of Closed Processes Based Cycle Powered by A Reversible Heat Pump that Exceed Carnot Factor | JOURNAL OF ADVANCES IN PHYSICS (rajpub.com); https://rajpub.com/index.php/jap/article/view/8034;

[23] Ramón Ferreiro Garcia. Efficient disruptive power plant-based heat engines doing work by means of strictly isothermal closed processes. Journal of Advances in Physics Vol 22 (2024), p 30.53, ISSN: 2347-3487. https://rajpub.com/index.php/jap/article/view/9587. https://doi.org/10.24297/jap.v15i0.9587.

[24] E. W. Lemmon, M. L. Huber, M. O. McLinden, NIST Reference Fluid Thermodynamic and Transport Properties - REFPROP Version 8.0, User's Guide, NIST, Boulder, CO. 2007.